HIGH-THROUGHPUT SCREENING USING DESIGNED SURROGATES FOR FATTY ALDEHYDE REDUCTASE ENGINEERING

SUPHANIDA WORAKAENSAI

A Thesis Submitted in Partial Fulfillment of the Requirements for the
Degree of Master of Science in Biochemistry and Biochemical Technology
Suranaree University of Technology
Academic Year 2022

ไฮทรูพุทสกรีนนิงโดยใช้สารตัวแทนที่ถูกออกแบบสำหรับการวิศวกรรมเอนไซม์แฟททีแอลดีไฮด์รีดักเตส

นางสาวศุภนิดา วรแก่นทราย

วิทยานิพนธ์นี้เป็นส่วนหนึ่งของการศึกษาตามหลักสูตรปริญญาวิทยาศาสตรมหาบัณฑิต
สาขาวิชาชีวเคมีและเทคโนโลยีชีวเคมี
มหาวิทยาลัยเทคโนโลยีสุรนารี
ปีการศึกษา 2565

HIGH-THROUGHPUT SCREENING USING DESIGNED SURROGATES FOR FATTY ALDEHYDE REDUCTASE ENGINEERING

Suranaree University of Technology has approved this thesis submitted in partial fulfillment of the requirements for a Master's Degree.

Thesis Examining Committee

(Prof. Dr. James R. Ketudat-Cairns)
Chairperson

(Asst. Prof. Dr. Rung-Yi Lai)
Member (Thesis Advisor)

(Asst. Prof. Dr. Anyanee Kamkaew)
Member

(Dr. Ratana Charoenwattanasatien)
Member

(Assoc. Prof. Dr. Chatchai Jothityangkoon)
Vice Rector for Academic Affairs
and Quality Assurance

(Prof. Dr. Santi Maensiri)
Dean of the Institute of Science

ศุภนิดา วรแก่นทราย : ไฮทรูพุทสกรีนนิงโดยใช้สารตัวแทนที่ถูกออกแบบสำหรับการวิศวกรรมเอนไซม์แฟททีแอลดีไฮด์รีดักเตส (HIGH-THROUGHPUT SCREENING USING DESIRED SURROGATES FOR FATTY ALDEHYDE REDUCTASE ENGINEERING) อาจารย์ที่ปรึกษา : ผู้ช่วยศาสตราจารย์ ดร.รุ่ง-ยี ไลย์, 84 หน้า.

คำสำคัญ: ไขมันแอลกอฮอล์ ไขมันแอลดีไฮด์รีดักเตส ไฮทรูพุทสกรีนนิง การวิศวกรรมโคเอนไซม์

ไขมันแอลกฮอล์คือสารตั้งต้นของอุตสาหกรรมที่สำคัญมากซึ่งส่วนใหญ่ถูกผลิตมาจากเชื้อเพลิงฟอสซิล อย่างไรก็ตาม การใช้เชื้อเพลิงฟอสซิลเป็นระยะเวลายาวนานได้สร้างความกังวลเป็นอย่างมากเกี่ยวกับการลดลงของเชื้อเพลิงฟอสซิลและภาวะโลกร้อน เพื่อที่จะจัดการกับปัญหาเหล่านี้ นักวิทยาศาสตร์ใช้ชีววิทยาสังเคราะห์เพื่อวิศวกรรมจุลินทรีย์ในการผลิตไขมันแอลกอฮอล์ ขั้นตอนสุดท้ายของชีวสังเคราะห์ของไขมันแอลกอฮอล์คือการรีดิวซ์ไขมันแอลดีไฮด์เป็นไขมันแอลกอฮอล์ที่เร่งปฏิกิริยาโดยไขมันแอลดีไฮด์รีดักเตส การเพิ่มกิจกรรมของไขมันแอลดีไฮด์รีดักเตสคือหนึ่งวิธีเพื่อให้ผลผลิตของไขมันแอลกอฮอล์เพิ่มขึ้น วิธีการพื้นฐานสำหรับใช้ตรวจสอบกิจกรรมของไขมันแอลดีไฮด์รีดักเตสคือการดูการลดลงของ NAD(P)H โดยใช้เครื่องสเปคโตร UV-Vis ที่ 340 นาโนเมตร ซึ่งวิธีนี้ใช้แรงงานที่มากและใช้เวลานานทำให้ไม่เหมาะสมสำหรับไฮทรูพุทสกรีนนิง วิทยานิพนธ์นี้ได้พัฒนาสารตัวแทนของไขมันแอลดีไฮด์สำหรับไฮทรูพุทสกรีนนิงของไขมันแอลดีไฮด์รีดักเตส สารตัวแทนของเฮกซานาลและออคทานาลคือ T6 และ T8 ซึ่งมีหมู่ฟอร์มิลไธโอเอสเทอร์ สารตัวแทนสามารถถูกรีดิวซ์โดยไขมันแอลดีไฮด์รีดักเตส YahK จากนั้นเกิดเป็นฟอร์มาลดีไฮด์ ฟอร์มาลดีไฮด์ที่เกิดขึ้นนั้นสามารถทำปฏิกิริยากับสารเพอพาล์ดแล้วให้เป็นสารที่มีสีม่วงซึ่งสามารถมองเห็นได้ด้วยตาหรือหาปริมาณได้ด้วยวัดการดูดกลืนแสงช่วง 550 นาโนเมตร เพื่อสาธิตการใช้ประโยชน์ของสารตัวแทนนี้ ผู้วิจัยประสบความสำเร็จในการประยุกต์สารตัว T6 เพื่อคัดกรอง library ของ YahK ที่เกิดการกลายจำนวน 2 variants ที่มีความจำเพาะต่อ NADH เพิ่มขึ้นเมื่อเปรียบเทียบกับ wild type ของ YahK

สาขาวิชาเคมี
ปีการศึกษา 2565

ลายมือชื่อนักศึกษา ศุภนิดา วรแก่นทราย
ลายมือชื่ออาจารย์ที่ปรึกษา Rung-Yi Lai

SUPHANIDA WORAKAENSAI : HIGH-THROUGHPUT SCREENING USING DESIGNED SURROGATES FOR FATTY ALDEHYDE REDUCTASE ENGINEERING. THESIS ADVISOR : ASST. PROF. RUNG-YI LAI, Ph.D. 84 PP.

Keywords: Fatty alcohol, Fatty aldehyde reductase, High-throughput screening, Coenzyme engineering

Fatty alcohols are crucial industrial precursors majorly produced from fossil fuels. However, long-term usage of fossil fuels generates substantial concerns about fossil fuel depletion and global warming. Researchers used synthetic biology to engineer microorganisms to produce fatty alcohols to overcome these issues. The last step of fatty alcohol biosynthesis is to reduce a fatty aldehyde to the corresponding fatty alcohol, which is catalyzed by fatty aldehyde reductase (FALR). To achieve higher yields of fatty alcohol, improvement of FALR activity is one approach. The standard assay to characterize FALR activity is to monitor NAD(P)H consumption by purified FALR by UV-Vis spectroscopy at 340 nm. This is laborious and time-consuming, making it unsuitable for high-throughput screening (HTS). This thesis developed the fatty aldehyde surrogates for HTS of FALR. The surrogates of hexanal and octanal are T6 and T8, which contain a formyl thioester group. The surrogates were reduced by *E. coli* YahK to generate formaldehyde. The resulting formaldehyde was derivatized by Purpald to yield a purple adduct, which is simply observed by the naked eye or quantified by UV-vis spectroscopy at 550 nm. To demonstrate the applicability of the surrogates, I successfully applied the surrogate T6 to screen a YahK FALR library to identify two variants with improved NADH specificities compared to YahK wild type preferring NADPH.

School of Chemistry
Academic Year 2022

Student's Signature สุภนิดา วรแก่นทราย
Advisor's Signature Rung-Yi Lai

ACKNOWLEDGEMENTS

I would like to express my deep appreciation to Asst. Prof. Dr. Rung-Yi Lai, my thesis advisor, for his patience, kind support, guidance, discussion, and encouragement throughout my thesis. Besides the advisor, I would like to acknowledge Prof. Dr. James R. Ketudat-Cairns, Asst. Prof. Dr. Anyanee Kamkaew, and Dr. Ratana Charoenwattanasatien for contributing to the thesis-examining committees. I would like to thank the group of Prof. Dr. James R. Ketudat-Cairns for suggesting molecular techniques, and the group of Asst. Prof. Dr. Anyanee Kamkaew for helping me to synthesize surrogate substrates. I am also extremely grateful to the Development and Promotion of Science and Technology Talents Project (DPST, THAILAND) for the scholarship during my master's degree program. In addition, this research and innovation activity is funded by National Research Council of Thailand (NRCT) and Suranaree University of Technology (SUT). I am also extending my special thanks to Dr. Utumporn Ngivprom who greatly suggested research methodology and several lab techniques. Finally, I would like to express thanks to my family and my boyfriend for their love, kind support, and encouragement.

Suphanida Worakaensai

CONTENTS

CONTENTS (Continued)

LIST OF TABLES

LIST OF FIGURES

Figure **Page**

LIST OF FIGURES (Continued)

LIST OF ABBREVIATIONS

FALR	Fatty aldehyde reductase
NAD^+	Oxidized nicotinamide adenine dinucleotide
NADH	Reduced nicotinamide adenine dinucleotide
$NADP^+$	Oxidized nicotinamide adenine dinucleotide phosphate
NADPH	Reduced nicotinamide adenine dinucleotide phosphate
UV-Vis	Ultraviolet-Visible
HTS	High-throughput screening
A6	Hexanal
A8	Octanal
T6	Surrogate of hexanal
T8	Surrogate of octanal
*Pa*FDH-WT	Wilde-type *Pseudomonas* sp. 101 formate dehydrogenase
*Pa*FDH-V9	Mutated *Pseudomonas* sp. 101 formate dehydrogenase
ACR	Fatty acyl-CoA reductase
ACP	Acyl carrier protein
CAR	Carboxylic acid reductase
PD	Pyruvate dehydrogenase
ACC	Acetyl-CoA carboxylase
TE	Thioesterase
FadD	Fatty acyl-CoA synthetase
afFAR	Alcohol-forming fatty acyl-CoA reductase
NMN^+	Nicotinamide mononucleotide
NBT	Nitroblue tertrazolium
PMS	Phenazine methosulfate
PCR	Polymerase chain reaction
*Ba*GDH	*Bacillus amyloliquefaciens* SB5 glucose dehydrogenase

LIST OF ABBREVIATIONS (Continued)

°C	Degrees Celsius
IPTG	Isopropyl-β-D-1-thiogalactopyranoside
DTNB	5,5'-Dithiobis-2-Nitrobenzoic Acid
SDS-PAGE	Sodium dodecyl-sulfate polyacrylamide gel electrophoresis
kDa	Kilodalton

CHAPTER I

INTRODUCTION

1.1 Background and significance

Fatty alcohols are one of the industrial precursors for detergents, pharmaceuticals, cosmetics, personal care products, lubricants, and promising biofuel substitutes (Cao *et al*., 2015; Cordova *et al*., 2020; McNeil and Stuart, 2018; Stephanopoulos, 2007). The industrial chemical processes of fatty alcohol synthesis use either renewable sources, such as oils and fats, or petrochemical sources. Both means generate substantial concerns about competition with food supplies, limited availability of fossil fuels, environmental issues, and global warming (Liu *et al*., 2014; Mudge, 2005). Furthermore, the current Coronavirus Disease 2019 (Covid-19) pandemic increases the demand for cleaning products, thus requiring more fatty alcohol production (Catton, 2020; Munkajohnpong *et al*., 2020). Therefore, sustainable and environmentally friendly processes for fatty alcohol production may overcome these concerns.

Producing fatty alcohols using microbes with an engineered fatty acid biosynthetic pathway (Akhtar *et al*., 2013) would be a promising alternative approach to the current chemical methods, since it utilizes low-cost materials and can control the chain length distribution of fatty alcohol using a chain length specific reductase (Youngquist *et al*., 2013). The last step of fatty alcohol biosynthesis is to reduce a fatty aldehyde to the corresponding fatty alcohol. The enzyme catalyzing this reduction is fatty aldehyde reductase (FALR). FALR belongs to one group of oxidoreductases, which mostly need to bind coenzymes, such as nicotinamide adenine dinucleotide (NAD, including NAD^+ and NADH) or its phosphorylated equivalent, nicotinamide adenine dinucleotide phosphate (NADP, including $NADP^+$ and NADPH), to catalyze reactions (Chánique and Parra, 2018; Pick *et al.*, 2012, 2014). Although this biological process has

fatty alcohol yield than the chemical processes, researchers have spent huge effort developing metabolic engineering and synthetic biology strategies to improve yield to meet industrial demand (Mehrer *et al*., 2018; Munkajohnpong *et al*., 2020; Youngquist *et al*., 2013).

To achieve higher yields of fatty alcohols, improvement of FALR activity is one approach. Most FALRs strongly prefer NADPH over NADH as the coenzyme (Pick *et al*., 2012; Rodriguez and Atsumi, 2014). This creates a vast challenge for the utilizing FALR in industrial processes and cell-free biosynthesis since NADPH is much more expensive ($168/100 mg for NADPH and $25/100 mg for NADH (TCI Chemicals)) and less stable (Beier *et al*., 2016; Chánique and Parra, 2018). Given the cost of NADPH, its stoichiometric use at a large scale is not economically feasible (Wang *et al*., 2020). Thus, coenzyme preference engineering of FALRs to switch from NADPH to NADH could be one strategy to reduce the cost of fatty alcohol production.

Coenzyme preference engineering is one popular area of protein engineering. One powerful engineering strategy is to conduct directed evolution or semi-rational design. The success of both engineering campaigns relies greatly on high-throughput screening (HTS) methods, which can rapidly and correctly identify benign mutants in a large library (Xiao *et al*., 2015; You *et al*., 2017). The standard method to characterize FALR is to monitor the NADPH consumption by purified FALR at 340 nm by UV-Vis spectroscopy (Fatma *et al*., 2016; Willis *et al*., 2011). This is laborious and time-consuming, involving protein purification and *in vitro* enzymatic assays. Furthermore, this method is difficult to apply in crude lysates containing FALR owing to the interference of cell lysate absorption signals. Therefore, this approach is not ideal for HTS (Mayer and Arnold, 2002). Faster and effective HTS approaches of FALR activity in whole cell or crude lysate assays remain to be discovered.

In this thesis, I propose fatty aldehyde surrogates capable of displaying color at the end of the assay for high-throughput screening of FALR. The surrogates, **T6** and **T8**, of fatty aldehydes, hexanal (**A6**) and octanal (**A8**), respectively, containing the formyl thioester group, could be reduced by FALR to generate formaldehyde. The resulting

formaldehyde was then derivatized by Purpald to yield a purple adduct, which could be observed by the naked eye or UV-Vis spectroscopy at 550 nm (Figure 1.1). To demonstrate the feasibility of the screening platform, this study applied the surrogate **T6** in high-throughput screening for coenzyme specificity engineering of *E. coli* YahK from NADPH to NADH. In addition, to reduce the stoichiometric NADH usage in HTS assays, *Pseudomonas* sp. 101 formate dehydrogenase (*Pa*FDH-WT) was used to catalyze the regeneration of NADH by formate oxidation (Figure 1.2).

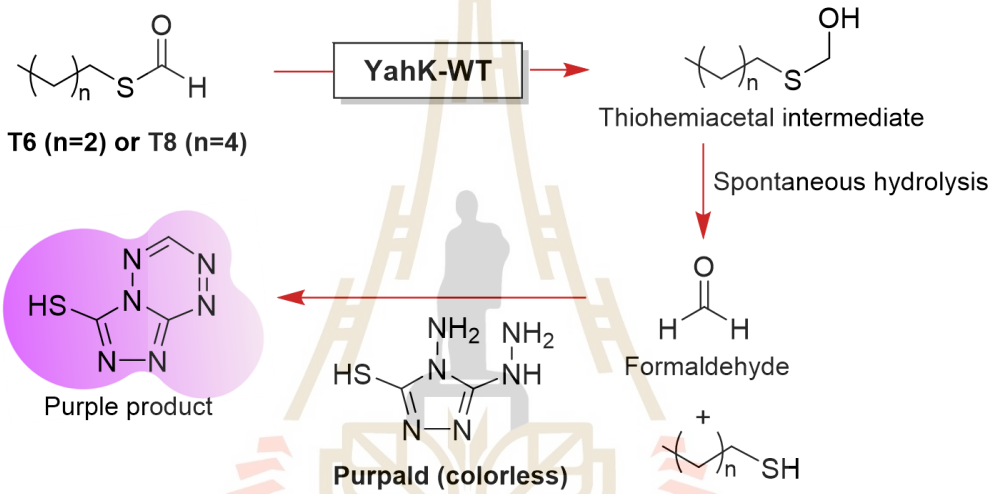

Figure 1.1 YahK-WT catalyzes the reduction of fatty aldehyde surrogate **T6** or **T8** containing formyl thioester group to form formaldehyde via a thiohemiacetal intermediate. The resulting formaldehyde is derivatized by Purpald to generate a purple product.

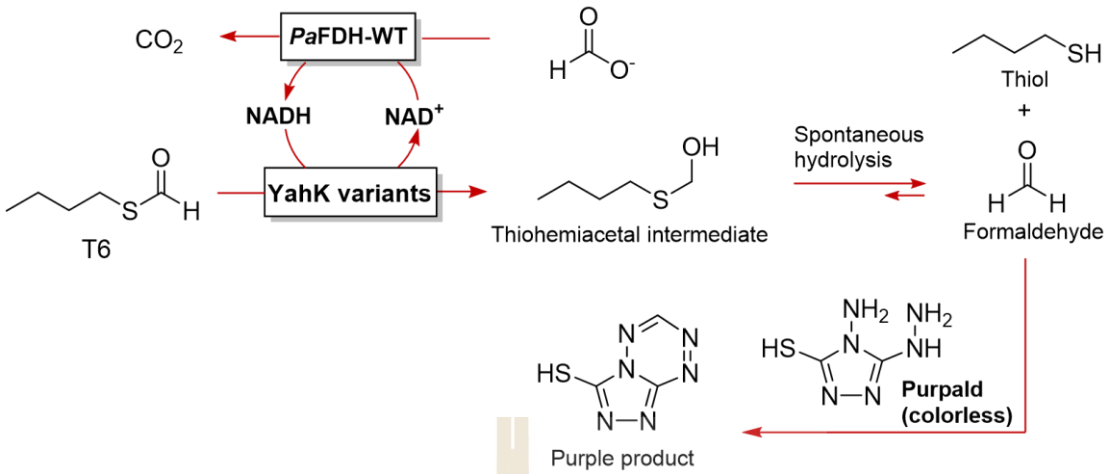

Figure 1.2 Platform design for HTS of FALR variants using NADH. The surrogate **T6** is reduced by YahK variants using NADH, which is regenerated by a coenzyme regeneration system catalyzed by *Pa*FDH-WT.

1.2 Research objectives

1) To test whether fatty aldehyde surrogates **T6** and **T8** can be reduced by YahK
2) To investigate whether formaldehyde is generated from **T6** and **T8** reductions catalyzed by YahK
3) To incorporate the coenzyme regeneration system into the YahK-catalyzed reaction
4) To demonstrate the feasibility of the surrogate **T6** in high-throughput screening for YahK engineering

1.3 Scope and limitations

1) Fatty aldehyde surrogates **T6** and **T8** were designed for high-throughput screening (HTS) of YahK engineering.
2) The feasibility of the surrogate **T6** in HTS was demonstrated by switching coenzyme specificity from NADPH to NADH.
3) The HTS method was carried out in 96-well plates.
4) Molecular modeling using the software AutoDock Vina was used to identify the mutation sites of YahK.

1.4 References

Akhtar, M. K., Turner, N. J., and Jones, P. R. (2013). Carboxylic acid reductase is a versatile enzyme for the conversion of fatty acids into fuels and chemical commodities. *Proceedings of the National Academy of Sciences*, *110*(1), 87.

Beier, A., Bordewick, S., Genz, M., Schmidt, S., van den Bergh, T., Peters, C., Joosten, H.-J., and Bornscheuer, U. T. (2016). Switch in Cofactor Specificity of a Baeyer-Villiger Monooxygenase. *Chembiochem : A European Journal of Chemical Biology*, *17*(24), 2312–2315.

Cao, Y. X., Xiao, W. H., Liu, D., Zhang, J. L., Ding, M. Z., and Yuan, Y. J. (2015). Biosynthesis of odd-chain fatty alcohols in *Escherichia coli*. *Metabolic Engineering*, *29*.

Catton, H. (2020). Global challenges in health and health care for nurses and midwives everywhere. *International Nursing Review*, *67*(1), 4–6.

Chánique, A., and Parra, L. (2018). Protein Engineering for Nicotinamide Coenzyme Specificity in Oxidoreductases: Attempts and Challenges. *Frontiers in Microbiology*, *9*.

Cordova, L. T., Butler, J., and Alper, H. S. (2020). Direct production of fatty alcohols from glucose using engineered strains of *Yarrowia lipolytica*. *Metabolic Engineering Communications*, *10*, e00105.

Fatma, Z., Jawed, K., Mattam, A., and Yazdani, S. S. (2016). Identification of long chain specific aldehyde reductase and its use in enhanced fatty alcohol production in E. coli. *Metabolic Engineering*, *37*.

Liu, R., Zhu, F., Lu, L., Fu, A., Lu, J., Deng, Z., and Liu, T. (2014). Metabolic engineering of fatty acyl-ACP reductase-dependent pathway to improve fatty alcohol production in *Escherichia coli*. *Metabolic Engineering*, *22*, 10–21.

Mayer, K. M., and Arnold, F. H. (2002). A Colorimetric Assay to Quantify Dehydrogenase Activity in Crude Cell Lysates. *Journal of Biomolecular Screening*, *7*(2), 135–140.

McNeil, B. A., and Stuart, D. T. (2018). Optimization of C16 and C18 fatty alcohol production by an engineered strain of *Lipomyces starkeyi*. *Journal of Industrial Microbiology and Biotechnology*, *45*(1), 1–14.

Mehrer, C. R., Incha, M. R., Politz, M. C., and Pfleger, B. F. (2018). Anaerobic production of medium-chain fatty alcohols via a β-reduction pathway. *Metabolic Engineering*, *48*, 63–71.

Mudge, S. (2005). Fatty Alcohols – a review of their natural synthesis and environmental distribution. *Executive Summary of the Soap and Detergent Association*.

Munkajohnpong, P., Kesornpun, C., Buttranon, S., Jaroensuk, J., Weeranoppanant, N., and Chaiyen, P. (2020). Fatty alcohol production: An opportunity of bioprocess. *Biofuels, Bioproducts and Biorefining*, *14*(5), 986–1009.

Pick, A., Ott, W., Howe, T., Schmid, J., and Sieber, V. (2014). Improving the NADH-cofactor specificity of the highly active AdhZ3 and AdhZ2 from *Escherichia coli* K-12. *Journal of Biotechnology*, *189*, 157–165.

Pick, A., Rühmann, B., Schmid, J., and Sieber, V. (2012). Novel CAD-like enzymes from *Escherichia coli* K-12 as additional tools in chemical production. *Applied Microbiology and Biotechnology*, *97*.

Rodriguez, G., and Atsumi, S. (2014). Toward aldehyde and alkane production by removing aldehyde reductase activity in *Escherichia coli*. *Metabolic Engineering*, *25*.

Stephanopoulos, G. (2007). Challenges in Engineering Microbes for Biofuels Production. *Science*, *315*(5813), 801.

Wang, W., Knoshaug, E. P., Wei, H., Van Wychen, S., Lin, C.-Y., Wall, T. V., Xu, Q., Himmel, M. E., and Zhang, M. (2020). High titer fatty alcohol production in *Lipomyces starkeyi* by fed-batch fermentation. *Current Research in Biotechnology*, *2*, 83–87.

Willis, R. M., Wahlen, B. D., Seefeldt, L. C., and Barney, B. M. (2011). Characterization of a Fatty Acyl-CoA Reductase from *Marinobacter aquaeolei* VT8: A Bacterial Enzyme Catalyzing the Reduction of Fatty Acyl-CoA to Fatty Alcohol. *Biochemistry*, *50*(48), 10550–10558.

Xiao, H., Bao, Z., and Zhao, H. (2015). High Throughput Screening and Selection Methods for Directed Enzyme Evolution. *Industrial & Engineering Chemistry Research*, *54*(16), 4011–4020.

You, C., Huang, R., Wei, X., Zhu, Z., and Zhang, Y.-H. P. (2017). Protein engineering of oxidoreductases utilizing nicotinamide-based coenzymes, with applications in synthetic biology. *Synthetic and Systems Biotechnology*, *2*(3), 208–218.

Youngquist, J. T., Schumacher, M. H., Rose, J. P., Raines, T. C., Politz, M. C., Copeland, M. F., and Pfleger, B. F. (2013). Production of medium chain length fatty alcohols from glucose in *Escherichia coli*. *Metabolic Engineering*, *20*, 177–186.

CHAPTER II

LITERATURE REVIEW

2.1 Fatty alcohol definitions and applications

Fatty alcohols are amphiphilic molecules containing hydrophobic hydrocarbon chains and a hydrophilic hydroxyl group, generally at the terminal position (Figure 2.1). The chemical and physical properties of fatty alcohols depend on their structures, such as the numbers of carbon atoms and the nature of the linear or branched hydrocarbon chain, the position and numbers of hydroxyl groups, and the numbers of unsaturated C=C double bonds (Hambalko *et al*., 2021; Mudge, 2005; Valoppi *et al*., 2018). Their property differences provide for widely different applications.

Fatty alcohols are widely used as industrial precursors for detergents (Thakur and Kundu, 2016), plasticizers (Vieira *et al*., 2011), and lubricants (Munkajohnpong *et al*., 2020) (Table 2.1). Furthermore, fatty alcohols are an additive in gasoline to improve its stability and performance (Fortman *et al*., 2008). Also, fatty alcohols can serve as precursors for alkyl ether-linked lipids and wax esters (Rizzo *et al*., 1987). Grand View Research, Inc. (2015) expected the market demand for fatty alcohols to be over 3 million tons by 2022. The Market Research Report (2020) also projected the global market size of the fatty alcohol market to reach USD 7.4 billion by 2027 with a composed annual growth rate (CAGR) of 5.2%. With the increasing demand for fatty alcohol, its production must keep pace.

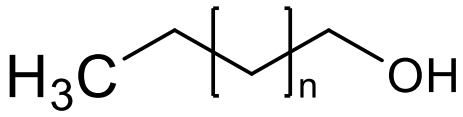

Figure 2.1 General structure of fatty alcohol. The value of the n component normally varies between 6 and 22. The hydroxyl group (-OH) usually presents in the primary position (Mudge, 2005; Valoppi *et al*., 2018).

Table 2.1 Applications of fatty alcohols with different chain lengths.

Applications	Hydrocarbon chain character	Reference
Detergents	Linear chain with a carbon chain length of at least 12 atoms	Thakur and Kundu, 2016
Lubricants	Linear or branched chain with a carbon chain length of 12-30 atoms (C_{12}-C_{30})	Munkajohnpong *et al*., 2020
Plasticizers	Straight or branched chain with 6-11 carbon atoms chain length (C_6-C_{11})	Vieira *et al*., 2011
Energy storage	C_{14}, C_{16}, and C_{18} with a high melting point	Carareto *et al*., 2014

2.2 Fatty alcohol synthesis

2.2.1 Current industrial fatty alcohol production

Currently, industrial production of fatty alcohols depends on either renewable sources, such as natural oils (plant oils or animal-based fats), or petrochemical sources, such as olefins and paraffins. The processes of fatty alcohols synthesis depend on the raw materials, with different chain lengths (Noweck and Grafahrend, 2006). In 2015, the global fatty alcohols production came from petrochemical sources around 27.6% in North America, while another 72.4% of the fatty alcohols produced was from renewable sources mainly in Asia (Munkajohnpong *et al*., 2020).

Fatty alcohols from renewable feedstocks are mainly produced from the hydrogenation of triglycerides in natural oils (Noweck and Grafahrend, 2006; Wang *et al*., 2016). Three main types of large-scale hydrogenation processes are slurry phase or suspension hydrogenation, gas-phase hydrogenation, and trickle-bed hydrogenation (Table 2.2) (Voeste and Buchold, 1984). Suspension hydrogenation is to convert fatty acid methyl esters or fatty acids to fatty alcohols whilst in gas-phase hydrogenation and trickle-bed hydrogenation, the common substrates for converting to fatty alcohols are fatty acid methyl esters and fatty acid wax esters (Noweck and Grafahrend, 2006).

The industrial method for fatty alcohol production from petrochemical feedstocks is called the Ziegler process. The first step is the hydrogenation of the starting materials (aluminum, hydrogen gas, and ethylene) to form triethylaluminum, followed by a chain growth reaction of ethylene into aluminum leading to alkyl groups with chain lengths ranging from C2 to C26. Finally, the resulting triethylaluminum is then oxidized to generate aluminum alkoxides, which are hydrolyzed to fatty alcohols (Behr, 2000; Wang, 2010).

These processes require high energy consumption, harsh conditions, and hazardous catalysts (Table 2.2). In addition, they have led to numerous issues, such as competition with food supplies, air pollution, fossil fuel source depletion, and anthropogenic climate change, promoting transmissions of infectious diseases, such as influenza (Catton, 2020; Hill *et al*., 2006; Liu *et al*., 2020). They currently also face the increasing price of raw materials (Zheng *et al*., 2012). Hence, exploring alternative approaches may yield both better and more environmentally friendly techniques.

Table 2.2 Synthetic conditions of fatty alcohols from renewable and petrochemical feedstocks (Noweck and Grafahrend, 2006; Thakur and Kundu, 2016; Voeste and Buchold, 1984; Wang, 2010).

Process condition	Renewable source			Petrochemical source
	Slurry phase hydrogenation	Gas-phase hydrogenation	Trickle-bed hydrogenation	Ziegler process
Temperature (°C)	250-300	200-240	180-220	60-150
Pressure (bar)	280	40	250-300	1-120
Catalyst	powder copper chromite	copper-zinc or copper-chromium mixed oxides	copper, chromium- or copper-zinc mixed oxides	Ziegler catalyst
Feedstock	methyl esters or fatty acids	fatty acid methyl esters or fatty acid wax esters	fatty acid methyl esters or fatty acid wax esters	aluminum, hydrogen gas, and ethylene

2.2.2 Alternative strategy for fatty alcohol production

Leveraging modern genetic techniques and synthetic biology allows researchers to engineer biosynthetic pathways in microorganisms to produce fatty alcohols (Youngquist *et al*., 2013). In bacteria, fatty alcohols are biosynthesized from fatty acids or fatty acid derivatives (fatty acyl-CoA, or fatty acyl carrier protein (ACP)). The production of fatty alcohol could be achieved by a two-step reduction (Figure 2.2). In the first step, fatty acyl-CoA reductase (ACR), acyl carrier protein (ACP) reductase (AAR), or carboxylic acid reductase (CAR) converts fatty acyl-CoA, fatty acyl-ACP, and free fatty acid to generate a fatty aldehyde. In the second step, fatty aldehyde reductase (FALR) then catalyzes the reduction of fatty aldehyde to form fatty alcohol. In addition, alcohol-forming fatty acyl-CoA reductases (afFAR), such as fatty acyl-CoA reductases from *Marinobacter aquaeolei* VT8 and jojoba (*Simmondsia chinensis*), have been found that are capable of four electrons reduction of fatty acyl-CoA to the corresponding fatty alcohol (Figure 2.2) (Fatma *et al*., 2016; Liu *et al*., 2014; Munkajohnpong *et al*., 2020; Wang *et al*., 2020).

The yields of fatty alcohols by the biological processes are lower than industrial processes. These bioprocesses, however, require less energy consumption and are more environmentally friendly without using metals and toxic catalysts. Furthermore, researchers have developed metabolic engineering strategies to engineer microorganisms, such as *Saccharomyces cerevisiae* (d'Espaux *et al*., 2017), *Yarrowia lipolytica* (Cordova *et al*., 2020), and *Escherichia coli* (Liu *et al*., 2016), and also applied protein engineering tools to enhance fatty alcohol production.

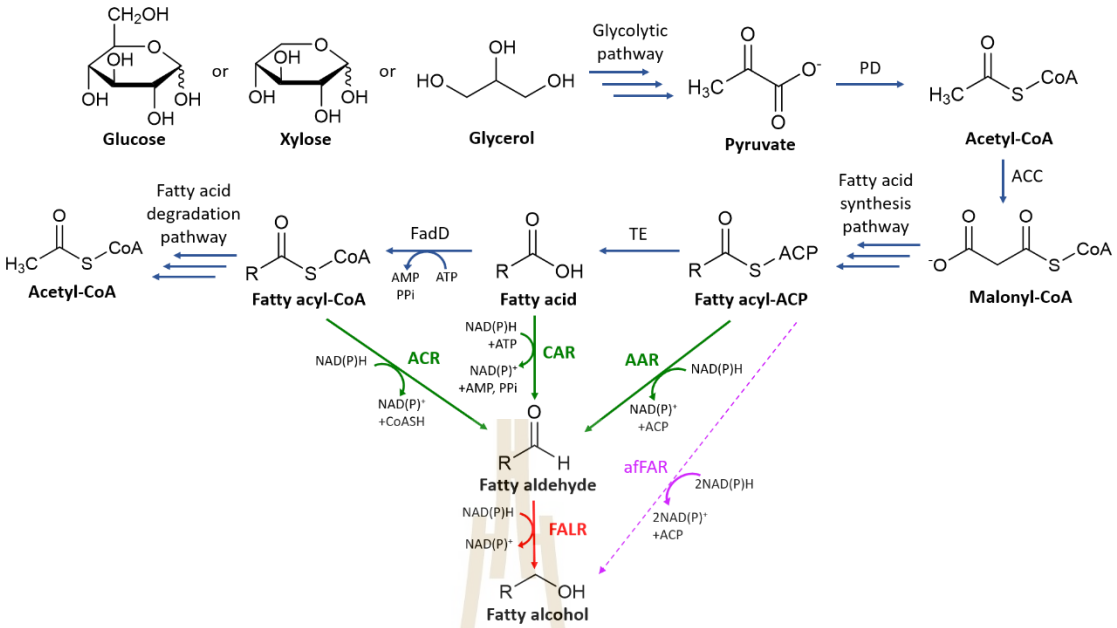

Figure 2.2 Engineered fatty alcohol biosynthetic pathway. In the two-enzyme reduction pathway, ACR, CAR, or AAR converts fatty acyl-CoA, fatty acid, and fatty acyl-ACP to fatty aldehyde as the intermediate, which is then reduced to fatty alcohol via FALR. afFAR reduces fatty acyl-CoA to form fatty alcohol. PD: pyruvate dehydrogenase; ACC: acetyl-CoA carboxylase; TE: thioesterase; FadD: fatty acyl-CoA synthetase; afFAR: alcohol-forming fatty acyl-CoA reductase; ACR: fatty acyl-CoA reductase; AAR: acyl carrier protein (ACP) reductase; CAR: carboxylic acid reductase; FALR: fatty aldehyde reductase. Modified from Fatma *et al.*, 2016; Liu *et al.*, 2014; Munkajohnpong *et al.*, 2020.

2.3 Fatty aldehyde reductase (FALR)

To improve fatty alcohols production, fatty acyl-CoA reductases were highly investigated and engineered. (Cordova *et al*., 2020; R. Liu *et al*., 2014; W. Wang *et al*., 2020; Yao *et al*., 2014; Youngquist *et al*., 2013). However, investigating FALR has not gained much interest for fatty alcohol production. FALR catalyzes the last step of fatty alcohol biosynthesis—reducing fatty aldehydes to fatty alcohols (Fatma *et al*., 2016). Rodriguez and Atsumi (2012) reported that fatty aldehyde reductases, AdhP, EutG, YiaY, YjgB, BetA, and FucO, contribute to generating isobutanol in engineered *E. coli*. Moreover, YahK and YbbO could reduce broad range of chain lengths of fatty aldehyde (acetaldehyde, isobutyraldehyde, hexanal, octanal, and decanal) while DkgA showed activities with medium chain length substrates (hexanal, and octanal) (Rodriguez and Atsumi, 2014). YahK, YjgB, YdhF, YqhD, and DkgA preferably utilize NADPH (reduced nicotinamide adenine dinucleotide phosphate) as the hydride source (Fatma *et al*., 2016; Jarboe, 2011; Pick *et al*., 2012). Moreover, in engineered *E. coli*, YjgB and YqhD overexpression can enhance fatty alcohol production (Cao *et al*., 2015). In addition, changing the cofactor specificity of FALRs (i.e., from NADPH to NADH or NADH to NADPH) could increase the production of fatty alcohol (Bommareddy *et al*., 2014).

FALRs are members of oxidoreductases, a large group of enzymes catalyzing hydride transfer from the cofactor, nicotinamide adenine dinucleotide, NAD^+/NADH, or nicotinamide adenine dinucleotide phosphate, $NADP^+$/NADPH, to substrates (Cahn *et al*., 2017; Chánique and Parra, 2018). The structures of these cofactors consist of two parts: the nicotinamide, serving as chemical functions (electron donor NAD(P)H or acceptor $NAD(P)^+$ by donating or accepting the hydride from or onto the C4 position); and the adenosine, containing the phosphate group for NADP or the hydroxyl group for NAD at the C2 position of the ribose (Figure 2.3) (Huang *et al*., 2019; Wang *et al*., 2019). Different structural motifs in enzyme active sites recognize NAD or NADP specifically. Generally, the negatively charged phosphate of NADP interacts with positively charged residues, especially arginine and hydrogen bond donating residues in NADP specific enzymes. The negatively charged residues in the active sites preferring NAD are prone to repel the phosphate group of NADP and interact with the 2'-OH and

3’-OH of the adenine ribose through hydrogen bonds. This specificity enables the cell to regulate different enzyme classes and pathways separately and prevent futile reaction cycles (Cahn *et al*., 2017; Chánique and Parra, 2018). To take into account the economic point of view in biocatalysis, NADH has a higher preference than NADPH, because NADH has higher stability and a much lower price (the bulk price for one mole: USD 3,000 for NADH and USD 215,000 for NADPH) (Beier *et al*., 2016; Chánique and Parra, 2018). Therefore, changing the coenzyme preference of FALRs is an attractive research area, which could be applied in biocatalysis and metabolic engineering (Chánique and Parra, 2018).

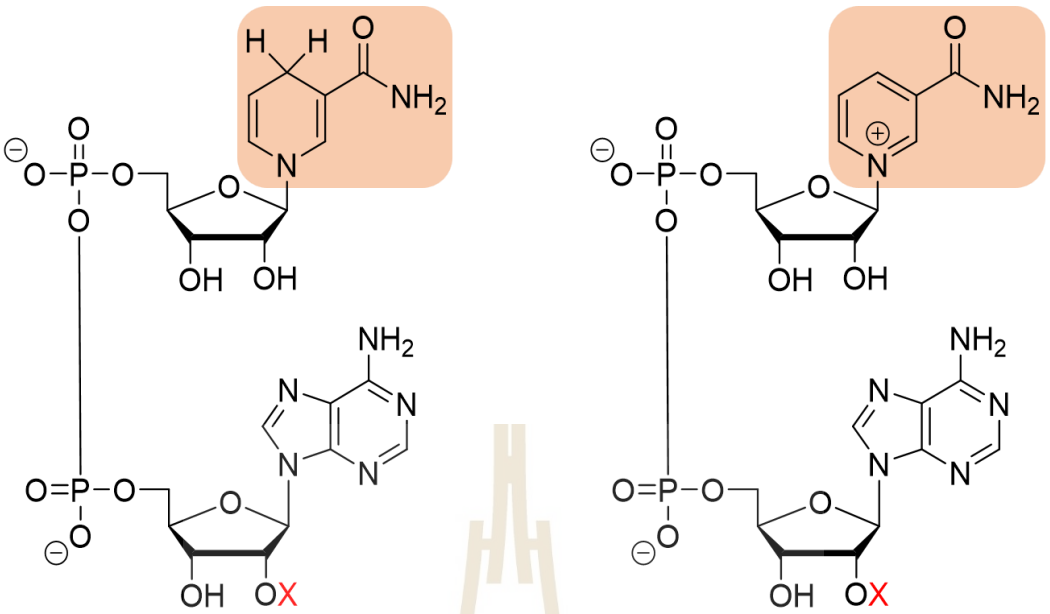

Figure 2.3 Chemical structures of NAD(P)H (reduced form) and $NAD(P)^+$ (oxidized form). The nicotinamide portion was highlighted in orange. The C2 position of the adenine portion contains the phosphate group (NADP) or hydroxyl group (NAD). The figure is modified from Paul *et al.*, 2014.

2.4 Coenzyme specificity engineering

Protein engineering is a tool to modify protein amino acid residues to obtain the desired properties, including enzyme activity improvement, thermostability, and coenzyme specificity. Coenzyme preference switch of oxidoreductases is a popular area of protein engineering. It plays a crucial role in pathway engineering and metabolic engineering *in vitro* and *in vivo*. Changing coenzyme preference from NAD to NADP or from NADP to NAD could promote coenzyme availability balance and cellular metabolism efficiency *in vivo* and also decrease the cost of *in vitro* production (Cahn *et al.*, 2017b; You *et al.*, 2017)

Three major strategies of engineering coenzyme specificity are rational design, directed evolution, and their combination (semi-rational strategy) (Figure 2.4). Rational

design is the conventional approach for switching cofactor preference to obtain mutants with improved properties. It requires in-depth knowledge of protein structure and structure-function relationship. The rational design process involves the identification of residue sites to be changed, usually relying upon protein crystallographic structure, and mutation of residues in active sites to certain other residues, which can be achieved through site-directed mutagenesis. Finally, mutated enzymes require characterization. This approach can be limited by the complexity of the structure-function relationship in enzymes. Even though the structure and catalytic mechanism of enzyme are well characterized, the mutation for the desired property is not directly predictable. (Chica *et al*., 2005; Percival *et al*., 2006; You *et al*., 2017).

Directed evolution is an alternative approach to engineering coenzyme preference without knowing the enzyme structure and interactions between enzyme and substrate (Liu *et al*., 2009). The two evolutionary methods used for *in vitro* directed evolution to generate a mutant library are random mutagenesis (e.g., error-prone PCR) and gene recombination (e.g., DNA shuffling) (Labrou, 2009). Semi-rational design is the combination of evolutionary methods of directed evolution with elements of rational design to overcome certain limitations of both tools. Semi-rational design targets multiple and specific residues to mutate based on enzyme structural and/or functional knowledge to create smarter libraries by saturation mutagenesis that are more feasible to yield positive results (Chica *et al*., 2005; You *et al*., 2017b).

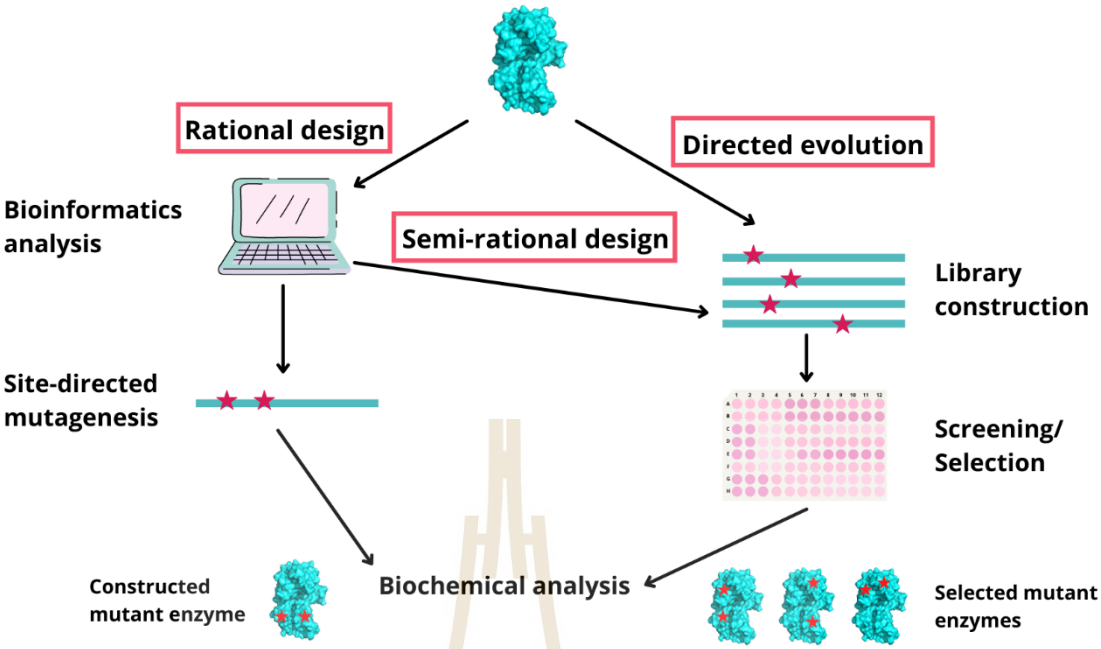

Figure 2.4 Schematic presentation of three coenzyme engineering strategies: rational design, semi-rational design, and directed evolution. This figure is modified from Percival *et al*., 2006; You *et al*., 2017.

2.5 High-throughput screening for coenzyme specificity engineering

The challenge of directed evolution and semi-rational approach is to develop methods, either selection or screening, that correctly and rapidly identify positive hits from diverse mutant libraries (You *et al*., 2017). Screening refers to the evaluation of each protein for finding the desired mutants, whereas selection automatically eliminates unwanted enzyme variants (Xiao *et al*., 2015). Although screening-based systems allow a noticeably lower throughput than selection approaches, screening methods are significantly more frequently used to find benign mutants. The two main screening approaches are (i) facilitated screening, which is carried out on solid agar to distinguish the positive mutants from the rest based on distinct phenotype, and (ii) random screening involves in picking mutants randomly for their performance evaluation (Percival *et al*., 2006).

The traditional approach to characterize FALR activity is to monitor the NAD(P)H consumption in the presence of FALR based on absorbance at 340 nm using UV-Vis spectroscopy (Fatma *et al*., 2016; Willis *et al*., 2011). This method slows down the engineering process, since researchers need to purify each variant from the mutant library to determine its activity *in vitro*. Brinkmann-Chen *et al*. (2013) modified such method *in vivo* by using cell lysates to find ketol-acid reductoisomerases with reversed cofactor preference from NADPH to NADH. However, this method is still unsuitable for high-throughput screening (HTS) in whole cell or crude lysate experiments, because of the strong absorption of UV light by cell lysate (moderate absorbance at 340 nm) (Mayer and Arnold, 2002). Several high-throughput screening (HTS) methods have been developed for nicotinamide coenzyme engineering of many oxidoreductases (Table 2.3), but HTS for coenzyme preference changing of FALR is still obscure. Thus, a simple, faster, and more effective HTS method for switching coenzyme preference of FALR needs exploration.

Table 2.3 High-throughput screening methods for coenzyme switching of oxidoreductase. NAD^+/NADH: nicotinamide adenine dinucleotide; $NADP^+$/NADPH: nicotinamide adenine dinucleotide phosphate; NMN^+: nicotinamide mononucleotide, NBT: nitroblue tertrazolium; PMS: phenazine methosulfate.

Enzyme	Altered property	Screening	Reference
Ketol-acid reductoisomerase	NADPH to NADH	Monitoring NAD(P)H consumption at 340 nm	Brinkmann-Chen *et al*., 2013
Lactate dehydrogenase	NAD^+ to $NADP^+$	Filter assay, followed by NBT-PMS assay	Flores and Ellington, 2005
Thermophilic 6-phosphogluconate dehydrogenase	$NADP^+$ to NAD^+	Peri-dish-based double-layer plus NBT-PMS assay	Huang *et al*., 2016
6-Phosphogluconate dehydrogenase	$NADP^+$ to NMN^+	NAD(P)-eliminated solid-phase assay (NESPA)	Huang *et al*., 2019

2.6 References

Behr, A. (2000). Ziegler Processes. *In Ullmann's Encyclopedia of Industrial Chemistry*, 1-4.

Beier, A., Bordewick, S., Genz, M., Schmidt, S., van den Bergh, T., Peters, C., Joosten, H.-J., and Bornscheuer, U. T. (2016). Switch in Cofactor Specificity of a Baeyer-Villiger Monooxygenase. *Chembiochem, 17*(24), 2312–2315.

Bommareddy, R. R., Chen, Z., Rappert, S., and Zeng, A.-P. (2014). A de novo NADPH generation pathway for improving lysine production of Corynebacterium glutamicum by rational design of the coenzyme specificity of glyceraldehyde 3-phosphate dehydrogenase. *Metabolic Engineering*, *25*, 30–37.

Brinkmann-Chen, S., Flock, T., Cahn, J. K. B., Snow, C. D., Brustad, E. M., McIntosh, J. A., Meinhold, P., Zhang, L., and Arnold, F. H. (2013). General approach to reversing ketol-acid reductoisomerase cofactor dependence from NADPH to NADH. *Proceedings of the National Academy of Sciences*, *110*(27), 10946.

Cahn, J. K. B., Werlang, C. A., Baumschlager, A., Brinkmann-Chen, S., Mayo, S. L., and Arnold, F. H. (2017a). A General Tool for Engineering the NAD/NADP Cofactor Preference of Oxidoreductases. *ACS Synthetic Biology*, *6*(2), 326–333.

Cahn, J. K. B., Werlang, C. A., Baumschlager, A., Brinkmann-Chen, S., Mayo, S. L., and Arnold, F. H. (2017b). A General Tool for Engineering the NAD/NADP Cofactor Preference of Oxidoreductases. *ACS Synthetic Biology*, *6*(2), 326–333.

Cao, Y.-X., Xiao, W.-H., Liu, D., Zhang, J.-L., Ding, M.-Z., and Yuan, Y.-J. (2015). Biosynthesis of odd-chain fatty alcohols in *Escherichia coli*. *Metabolic Engineering*, *29*.

Carareto, N. D. D., dos Santos, A. O., Rolemberg, M. P., Cardoso, L. P., Costa, M. C., and Meirelles, A. J. A. (2014). On the solid–liquid phase diagrams of binary mixtures of even saturated fatty alcohols: Systems exhibiting peritectic reaction. *Thermochimica Acta*, *589*, 137–147.

Catton, H. (2020). Global challenges in health and health care for nurses and midwives everywhere. *International Nursing Review*, *67*(1), 4–6.

Chánique, A., and Parra, L. (2018). Protein Engineering for Nicotinamide Coenzyme Specificity in Oxidoreductases: Attempts and Challenges. *Frontiers in Microbiology*, *9*.

Chica, R. A., Doucet, N., and Pelletier, J. N. (2005). Semi-rational approaches to engineering enzyme activity: Combining the benefits of directed evolution and rational design. *Protein Technologies and Commercial Enzymes*, *16*(4), 378–384.

Cordova, L. T., Butler, J., and Alper, H. S. (2020). Direct production of fatty alcohols from glucose using engineered strains of *Yarrowia lipolytica*. *Metabolic Engineering Communications*, *10*, e00105.

d'Espaux, L., Ghosh, A., Runguphan, W., Wehrs, M., Xu, F., Konzock, O., Dev, I., Nhan, M., Gin, J., Reider Apel, A., Petzold, C. J., Singh, S., Simmons, B. A., Mukhopadhyay, A., García Martín, H., and Keasling, J. D. (2017). Engineering high-level production of fatty alcohols by *Saccharomyces cerevisiae* from lignocellulosic feedstocks. *Metabolic Engineering*, *42*, 115–125.

Fatma, Z., Jawed, K., Mattam, A., and Yazdani, S. S. (2016). Identification of long chain specific aldehyde reductase and its use in enhanced fatty alcohol production in *E. coli*. *Metabolic Engineering*, *37*.

Flores, H., and Ellington, A. D. (2005). A modified consensus approach to mutagenesis inverts the cofactor specificity of *Bacillus stearothermophilus* lactate dehydrogenase. *Protein Engineering, Design and Selection*, *18*(8), 369–377.

Fortman, J. L., Chhabra, S., Mukhopadhyay, A., Chou, H., Lee, T. S., Steen, E., and Keasling, J. D. (2008). Biofuel alternatives to ethanol: Pumping the microbial well. *Trends in Biotechnology*, *26*(7), 375–381.

Hambalko, J., Gajdoš, P., Nicaud, J.-M., Ledesma-Amaro, R., Tupec, M., Pichová, I., and Čertík, M. (2021). Production of Long Chain Fatty Alcohols Found in Bumblebee Pheromones by *Yarrowia lipolytica*. *Frontiers in Bioengineering and Biotechnology*, *8*, 1498.

Hill, J., Nelson, E., Tilman, D., Polasky, S., and Tiffany, D. (2006). Environmental, Economic, and Energetic Costs, and Benefits of Biodiesel and Ethanol Biofuels.

Proceedings of the National Academy of Sciences of the United States of America, *103*, 11206–11210.

Huang, R., Chen, H., Upp, D. M., Lewis, J. C., and Zhang, Y.-H. P. J. (2019). A High-Throughput Method for Directed Evolution of NAD(P)$^+$-Dependent Dehydrogenases for the Reduction of Biomimetic Nicotinamide Analogues. *ACS Catalysis*, *9*(12), 11709–11719.

Huang, R., Chen, H., Zhong, C., Kim, J., and Zhang, Y.-H. P. (2016). High-Throughput Screening of Coenzyme Preference Change of Thermophilic 6-Phosphogluconate Dehydrogenase from NADP$^+$ to NAD$^+$. *Scientific Reports*, *6*, 32644.

Jarboe, L. R. (2011). YqhD: a broad-substrate range aldehyde reductase with various applications in production of biorenewable fuels and chemicals. *Applied Microbiology and Biotechnology*, *89*(2), 249–257.

Labrou, N. (2009). Random Mutagenesis Methods for *In Vitro* Directed Enzyme Evolution. *Current Protein and Peptide Science*, *11*.

Liu, Q., Tan, Z.-M., Sun, J., Hou, Y., Fu, C., and Wu, Z. (2020). Changing rapid weather variability increases influenza epidemic risk in a warming climate. *Environmental Research Letters*, *15*.

Liu, R., Zhu, F., Lu, L., Fu, A., Lu, J., Deng, Z., and Liu, T. (2014). Metabolic engineering of fatty acyl-ACP reductase-dependent pathway to improve fatty alcohol production in *Escherichia coli*. *Metabolic Engineering*, *22*, 10–21.

Liu, W., Hong, J., Bevan, D. R., and Zhang, Y.-H. P. (2009). Fast identification of thermostable beta-glucosidase mutants on cellobiose by a novel combinatorial selection/screening approach. *Biotechnology and Bioengineering*, *103*(6), 1087–1094.

Liu, Y., Chen, S., Chen, J., Zhou, J., Wang, Y., Yang, M., Qi, X., Xing, J., Wang, Q., and Ma, Y. (2016). High production of fatty alcohols in *Escherichia coli* with fatty acid starvation. *Microbial Cell Factories*, *15*(1), 129.

Mayer, K. M., and Arnold, F. H. (2002). A Colorimetric Assay to Quantify Dehydrogenase Activity in Crude Cell Lysates. *Journal of Biomolecular Screening*, *7*(2), 135–140.

Mudge, S. (2005). Fatty Alcohols – a review of their natural synthesis and environmental distribution. *Executive Summary of the Soap and Detergent Association*, *132*, 1-141.

Munkajohnpong, P., Kesornpun, C., Buttranon, S., Jaroensuk, J., Weeranoppanant, N., and Chaiyen, P. (2020). Fatty alcohol production: An opportunity of bioprocess. *Biofuels, Bioproducts and Biorefining*, *14*(5), 986–1009.

Noweck, K., and Grafahrend, W. (2006). Fatty Alcohols. In *Ullmann's Encyclopedia of Industrial Chemistry*, *14*, 117-141.

Paul, C. E., Arends, I. W. C. E., and Hollmann, F. (2014). Is Simpler Better? Synthetic Nicotinamide Cofactor Analogues for Redox Chemistry. *ACS Catalysis*, *4*(3), 788–797.

Percival Zhang, Y.-H., Himmel, M. E., and Mielenz, J. R. (2006). Outlook for cellulase improvement: Screening and selection strategies. *Biotechnology Advances*, *24*(5), 452–481.

Pick, A., Ott, W., Howe, T., Schmid, J., and Sieber, V. (2014). Improving the NADH-cofactor specificity of the highly active AdhZ3 and AdhZ2 from *Escherichia coli* K-12. *Journal of Biotechnology*, *189*, 157–165.

Pick, A., Rühmann, B., Schmid, J., and Sieber, V. (2012). Novel CAD-like enzymes from *Escherichia coli* K-12 as additional tools in chemical production. *Applied Microbiology and Biotechnology*, *97*.

Rizzo, W. B., Craft, D. A., Dammann, A. L., and Phillips, M. W. (1987). Fatty alcohol metabolism in cultured human fibroblasts. Evidence for a fatty alcohol cycle. *Journal of Biological Chemistry*, *262*(36), 17412–17419.

Rodriguez, G., and Atsumi, S. (2014). Toward aldehyde and alkane production by removing aldehyde reductase activity in *Escherichia coli*. *Metabolic Engineering*, *25*.

Rodriguez, G. M., and Atsumi, S. (2012). Isobutyraldehyde production from *Escherichia coli* by removing aldehyde reductase activity. *Microbial Cell Factories*, *11*(1), 90.

Thakur, D. S., and Kundu, A. (2016). Catalysts for Fatty Alcohol Production from Renewable Resources. *Journal of the American Oil Chemists' Society*, *93*(12), 1575–1593.

Valoppi, F., Calligaris, S., and Marangoni, A. G. (2018). Chapter 9—Stearyl Alcohol Oleogels. *Edible Oleogels (Second Edition)*, 219–234.

Vieira, M. G. A., da Silva, M. A., dos Santos, L. O., and Beppu, M. M. (2011). Natural-based plasticizers and biopolymer films: A review. *European Polymer Journal*, *47*(3), 254–263.

Voeste, T., and Buchold, H. (1984). Production of fatty alcohols from fatty acids. *Journal of the American Oil Chemists' Society*, *61*(2), 350–352.

Wang, G., Xiong, X., Ghogare, R., Wang, P., Meng, Y., and Chen, S. (2016). Exploring fatty alcohol-producing capability of *Yarrowia lipolytica*. *Biotechnology for Biofuels*, *9*(1), 107.

Wang, L., Liu, B., Liu, Y., Sun, Y., Liu, W., Yu, D., and Zhao, Z. K. (2019). *Escherichia coli* Strain Designed for Characterizing in Vivo Functions of Nicotinamide Adenine Dinucleotide Analogues. *Organic Letters*, *21*(9), 3218–3222.

Wang, W., Knoshaug, E. P., Wei, H., Van Wychen, S., Lin, C.-Y., Wall, T. V., Xu, Q., Himmel, M. E., and Zhang, M. (2020). High titer fatty alcohol production in *Lipomyces starkeyi* by fed-batch fermentation. *Current Research in Biotechnology*, *2*, 83–87.

Wang, Z. (2010). Ziegler Alcohol Synthesis. *In Comprehensive Organic Name Reactions and Reagents*, 3134–3138.

Willis, R. M., Wahlen, B. D., Seefeldt, L. C., and Barney, B. M. (2011). Characterization of a Fatty Acyl-CoA Reductase from *Marinobacter aquaeolei* VT8: A Bacterial Enzyme Catalyzing the Reduction of Fatty Acyl-CoA to Fatty Alcohol. *Biochemistry*, *50*(48), 10550–10558.

Xiao, H., Bao, Z., and Zhao, H. (2015). High Throughput Screening and Selection Methods for Directed Enzyme Evolution. *Industrial & Engineering Chemistry Research*, *54*(16), 4011–4020.

Yao, L., Qi, F., Tan, X., and Lu, X. (2014). Improved production of fatty alcohols in cyanobacteria by metabolic engineering. *Biotechnology for Biofuels*, *7*(1), 94.

You, C., Huang, R., Wei, X., Zhu, Z., and Zhang, Y.-H. P. (2017). Protein engineering of oxidoreductases utilizing nicotinamide-based coenzymes, with applications in synthetic biology. *Synthetic and Systems Biotechnology*, *2*(3), 208–218.

Youngquist, J. T., Schumacher, M. H., Rose, J. P., Raines, T. C., Politz, M. C., Copeland, M. F., and Pfleger, B. F. (2013). Production of medium chain length fatty alcohols from glucose in *Escherichia coli*. *Metabolic Engineering*, *20*, 177–186.

Zheng, Y.-N., Li, L.-L., Liu, Q., Yang, J.-M., Wang, X.-W., Liu, W., Xu, X., Liu, H., Zhao, G., and Xian, M. (2012). Optimization of fatty alcohol biosynthesis pathway for selectively enhanced production of C12/14 and C16/18 fatty alcohols in engineered *Escherichia coli*. *Microbial Cell Factories*, *11*(1), 65.

CHAPTER III

MATERIALS AND METHODS

3.1 Chemical, plasmid, and strain

Laboratory materials and preparation were performed in Asst. Prof. Dr.Rung-Yi Lai's lab and the Center of Science and Technological Equipment, Suranaree University of Technology. The surrogates **T6** and **T8** were synthesized by Asst. Prof. Anyanee Kamkaew's group. All chemicals were purchased from either Sigma-Aldrich or TCI Chemicals. Genomic DNA was purified by using a BioFact Genomic DNA Prep Kit. Oligonucleotides were purchased from Integrated DNA Technologies. DNA purification kits were purchased from Vivantis. All plasmids made were constructed by Gibson assembly of PCR products (Gibson *et al*., 2009). Strains, oligonucleotides, and plasmids are listed in Table 6.1, Table 6.2, and Table 6.3.

Table 3.1 List of strains used in this study.

Strains	Description	Reference
E. coli BL21 (DE3)	Host for protein expression	Invitrogen
E. coli MG1655	Strain for amplifying *YahK*	NIG in Japan
E. coli RARE	MG1655(DE3) Δ*dkgB*, Δ*yeaE*, Δ*yahK*, Δ*ygjB*, Δ*yqhC*, Δ*yqhD*, Δ*dkgA*	Addgene
B. amyloliquefaciens SB5	Strain for $NAD(P)^+$-dependent glucose dehydrogenase	Pongtharangkul *et al*., 2015
E. coli NEB® 5-alpha	Strain for storing plasmid	NEB

Table 3.2 List of oligonucleotides used in this study. Boldface nucleotide sequences indicate randomized positions and underlined nucleotide sequence is the priming site.

Primers	Sequence 5' -> 3'	Description
RYL013	GATCCGGCTGCTAACAAAG	Forward pET30a backbone
RYL020	CCCTGGAAGTACAGGTTCTC	Reverse pET30a backbone
RYL118	GAGAACCTGTACTTCCAGGGCGGTGGCATGAAGATCAAAGCTGTTGGTGC	Forward Ec*YahK*
RYL119	GCTTTGTTAGCAGCCGGATCTCAGTCTGTTAGTGTGCGATTATCG	Reverse Ec*YahK*
RYL154	GTATAAGAAGGAGATATACATATGTACACGGATTTAAAAGGAAAAGTCGTTGCC	Forward BaGDH
RYL155	ATCCGCGGCCTGCCTGGAAT	Reverse *BaGDH*
RYL156	CATTCCAGGCAGGCCGCGGATCAGGTGGCCATCACCATCACCATCACTAA	Forward pET-human-ferritin
RYL157	CATATGTATATCTCCTTCTTATACTTAACTAATATAC	Reverse pET-human-ferritin
RYL185	**NNK**TCTGAGGCAAAACGCGAAGC	Forward for mutagenesis
RYL186	**MNN**AAATGCCACCACATGTGCCC	Reverse for mutagenesis

Table 3.3 List of plasmids used in this study.

Plasmids	Description	Reference
pET30a	Plasmid for protein expression	Addgene
pET30a-*EcYahK*	pET30a containing *EcYahK* gene	This study
pET-*BaGDH*	pET-human-ferritin containing *BaGDH* gene	This study
pET28a-MBP-TEV	pET28a containing MBP-TEV gene	Addgene
pZ-ASL-PseFDH-V9	Plasmid containing FDH-V9 gene	Arren Bar-Even
pZ-ASL-PseFDH-WT	Plasmid containing FDH-WT gene	Arren Bar-Even

3.2 Plasmid construction

To make pET30a-*EcYahK*, the *EcYahK* gene was amplified from *E. coli* MG1655 using the primers RYL118 and RYL119 and the linearized vector backbone was amplified from pET30a using the primers RYL013 and RYL020. The plasmid pET30a-*BaGDH* was constructed as follows: the inserted *BaGDH* gene was amplified from *Bacillus amyloliquefaciens* SB5 genomic DNA using the primers RYL154 and RYL155 and the linearized vector backbone was amplified from pET-human-ferritin using RYL156 and RYL157 primers. All inserts and vector backbones were assembled by Gibson assembly (Gibson *et al*., 2009). After transformation into *E. coli* NEB® 5-alpha, the pET30-*EcYahK* and pET30-*BaGDH* plasmids were obtained.

For mutant library construction, saturation mutagenesis of the residues T205 and T206 was achieved by amplification from pET30a-*EcYahK* using the degenerate primers RYL185 and RYL186. The PCR reaction was carried out with NEB Phusion® DNA polymerase under the following condition: 98 °C denaturation for 30 s; 35 cycles of 98 °C denaturation for 10 s, 63 °C annealing for 20 s, and 72 °C extension for 4 min; and 72 °C extension for 5 min. The amplified PCR product was purified with a DNA purification kit (Vivantis) and phosphorylated by T4 kinase, followed by ligation by T4 ligase (New England Biolabs). Plasmid transformation into *E. coli* RARE was carried out by the heat-shock method (Singh *et al*., 2010).

3.3 Protein overexpression and purification

3.3.1 *Ec*YahK and *Ba*GDH overexpression and purification

A single colony of *E. coli* BL21(DE3) containing either pET30a-*EcYahK* or pET-*Ba*GDH was inoculated into 50 mL of Luria-Bertani broth (LB) containing 50 μg/mL kanamycin and grown overnight at 37 °C and 200 rpm. Ten milliliters of the overnight culture were inoculated into 1 L of LB with 50 μg/mL kanamycin and grown until OD_{600} reached about 0.6. The protein expression was induced by adding Isopropyl-β-D-1-thiogalactopyranoside (IPTG) to the final concentration of 200 μM and the culture

mixture was grown for 16 hr. at 200 rpm and 20 °C. The cells were collected by centrifugation at 8 °C and 5000 rpm for 25 min. The harvested cells were resuspended in the lysis buffer (300 mM NaCl, 50 mM NaH_2PO_4, and 10 mM Imidazole, pH 8.0). The cells were lysed by sonication (1.5 s cycle, 50% duty), followed by centrifugation at 4 °C and 12,000 rpm for 40 min. The supernatants were loaded onto the Ni-NTA column (QIAGEN) and the proteins were eluted by the manufacturer's instructions. After elution, the protein was desalted via a 10-DG column (BioRad) pre-equilibrated with 100 mM potassium phosphate buffer, 20% glycerol, pH7.5. The purified protein was stored in aliquots at -80 °C.

3.3.2 *Pa*FDH-WT and *Pa*FDH-V9 overexpression and purification

A single colony of *E. coli* BL21(DE3) harboring pZ-ASL-*Pse*FDH-WT or pZ-ASL-*Pse*FDH-V9 was inoculated into 50 mL of terrific broth containing 100 µg/mL streptomycin and grown overnight at 37 °C and 200 rpm. Ten milliliters of overnight culture were inoculated into 1 L of terrific broth with 100 µg/mL streptomycin. The culture was shaken at 200 rpm and 30 °C for an additional 16 hours. The cells were collected by centrifugation at 5000 rpm and 8 °C for 25 min. The cells were resuspended in buffer A (20 mM Tris, 500 mM NaCl, and 5 mM imidazole, pH 7.9). The cells were lysed by sonication for 30 s three times (1.5 s cycle, 50% duty) on ice, followed by centrifugation at 12,000 rpm and 4 °C for 40 min. The supernatant was applied to the Ni-NTA column (QIAGEN) and the protein was eluted by the manufacturer's instructions. After elution, the proteins were desalted through a 10-DG column (BioRad) pre-equilibrated with 100 mM Na_2HPO_4, pH 7.0. The purified proteins were stored in aliquots at -80 °C.

3.4 Enzymatic assay

All assays were carried out in a total volume of 1 mL. The assays were initiated by the addition of purified enzyme to the reaction mixture containing 100 μM of NAD(P)H, and 500 μM of **A6** (hexanal), **A8** (octanal), **T6**, or **T8** in 100 mM potassium phosphate buffer, pH 7.5. All assays were performed in triplicate at room temperature. The NAD(P)H consumption was measured at 340 nm with a NanoDrop 2000c spectrophotometer.

3.5 Purpald assay

For enzymatic experiment, the reactions were initiated by adding the purified enzyme to the reaction mixture containing 100 μM of NADPH, 500 μM of **T6** or **T8** in 100 mM potassium phosphate buffer, pH 7.5 with a final volume of 200 μL. For cell lysate experiment, the overnight culture of *E. coli* MG1655 RARE harboring pET30a-*EcYahK* or pET28a-MBP-TEV was inoculated LB with 50 μg/mL kanamycin and grown until OD_{600} reached about 0.6. The protein expression was induced by adding IPTG to the final concentration of 200 μM and the culture mixture was grown for 16 hr. After centrifugation to obtain the cell pellets, the harvested cells were lysed by 0.2 mg/mL lysozyme in 100 mM potassium phosphate buffer, pH 7.5, and the mixture was then incubated at 37 °C for 30 min. The cell lysate was centrifuged at 4000 rpm at 4 °C for 20 min to obtain the supernatant. The assays were initiated by the adding 100 μL of the supernatant to the reaction mixture containing 100 μM NADPH, 500 μM **T6**, and 100 mM potassium phosphate buffer, pH 7.5 to bring the final volume to 200 μL. All assays were incubated at room temperature for 10 min, followed by adding 50 μL of 100 mM Purpald solution (100 mM Purpald was prepared in 1 M NaOH). After incubating at room temperature aerobically for 15 min, the absorbance of the solution showing purple was measured at 550 nm using a microplate spectrophotometer (Thermo Scientific™ Multiskan™ GO). The formaldehyde amount was calculated by the calibration curve of the formaldehyde standard solution.

3.6 DTNB assay

For enzymatic experiment, all assays were carried out in a total volume of 200 µL. The reactions were initiated by adding 0.1 µM purified *Ec*YahK to the reaction mixture containing 100 mM potassium phosphate buffer, pH 7.5, 100 µM NADPH, 500 µM **T6** or **T8**, and 1 mM DTNB. For the cell lysate experiment, the harvested cells were lysed by 0.2 mg/mL lysozyme in 100 mM potassium phosphate buffer, pH 7.5, and the mixture was then incubated at 37 °C for 30 min. The cell lysate was centrifuged at 4000 rpm at 4 °C for 20 min to obtain the supernatant. The assays were initiated by adding 100 µL of the supernatant to the reaction mixture containing 100 mM potassium phosphate buffer, pH 7.5, 100 µM NADPH, 500 µM **T6** or **T8**, and 1 mM DTNB. The absorbance at 412 nm was measured at 0 min and after 10 min using a microplate spectrophotometer (Thermo Scientific™ Multiskan™ GO). The amount of produced thiol was calculated by the calibration curve of 1-butanethiol standard solution for **T6** and 1-hexanethiol for **T8**.

3.7 Kinetic constant determination

For determining apparent kinetic parameters on coenzymes, the reactions were carried out in 1 mL of 100 mM potassium phosphate buffer (pH 7.5) containing 0-300 µM NAD(P)H, and 500 µM **A6**. For the apparent kinetic parameters for NADPH, the enzyme concentrations of wild-type YahK, E3, and C8 were 5 nM. For the apparent kinetic parameters for NADH, the enzyme concentrations of wild-type YahK, E3, and C8 were 75 nM, 20 nM, and 50 nM, respectively. For the apparent kinetic parameters for the substrates (**A6**, **A8**, **T6**, and **T8**), the reactions were performed in 1 mL of 100 mM potassium phosphate buffer (pH 7.5) with the final concentration of 100 µM NADPH and 0-100 µM the substrate. The enzyme concentrations were 10 nM for **A6** and **A8** and 100 nM for **T6** and **T8**. NAD(P)H consumption was measured at 340 nm in 2 s intervals for 10 min on a NanoDrop 2000c spectrophotometer. Initial rates were calculated using the extinction coefficient of NAD(P)H (**ε** = 6.22 $mM^{-1}cm^{-1}$) with the linear initial slope of reaction. The apparent kinetic parameters, K_m and V_{max}, were

calculated by fitting the reaction rate and substrate concentration in nonlinear regression of the Michaelis–Menten curves with GraFit 5.0 (Erithacus Software, Horley, Survey, UK). The apparent k_{cat} was obtained by dividing V_{max} by the final enzyme concentration.

3.8 High-throughput screening of YahK engineering

For high-throughput screening assay, induced *E. coli* RARE cells harboring pET30a-*EcYahK*-NNK library or empty vector (pET28a-*MBP-TEV*; as control) in 96-well plates were harvested by centrifugation at 8 °C and 4000 rpm for 20 min. The harvested cells were lysed with 0.2 mg/mL lysozyme, followed by incubation at 37 °C for 30 min. The lysed cells were centrifuged at 4 °C and 4000 rpm for 20 min to remove the cell debris. One hundred microliters of supernatant was transferred to a new 96-well plate. Subsequently 100 µL of reaction mixture, containing 10 µM NAD^+, 10 mM formate, 500 µM **T6**, and 100 mM potassium phosphate buffer, pH 7.5, were added to each sample well. The 96-well plate was shaken for 20 min at room temperature. Fifty microliters of 100 mM Purpald in 1 M NaOH were then added to each sample well. After incubating for 15 min at room temperature in the presence of air, the intensity of purple product in each sample well was measured based on absorbance at 550 nm using a microplate spectrophotometer (Thermo Scientific™ Multiskan™ GO).

3.9 Modeling and docking analysis

The crystal structure of YahK (PDB: 1UUF) was used as the starting template (Pick *et al*., 2014). The NADPH ligand structure was downloaded from the PDB database (https://www.rcsb.org/). The ligand and receptor models were prepared with AutoDockTools. Docking of the ligand to wild-type YahK and mutants was performed in AutoDock vina (http://vina.scripps.edu/). Possible ligand conformations were generated by docking the NADPH ligand into the active site of wild-type and mutants. PyMOL was used for interaction viewing and image processing.

3.10 References

Gibson, D., Young, L., Chuang, R., Venter, J., Hutchison, C., and Smith, H. (2009). Enzymatic assembly of DNA molecules up to several hundred kilobas1. *Nature Methods*, *6*, 343–345.

Pick, A., Ott, W., Howe, T., Schmid, J., and Sieber, V. (2014). Improving the NADH-cofactor specificity of the highly active AdhZ3 and AdhZ2 from *Escherichia coli* K-12. *Journal of Biotechnology*, *189*, 157–165.

Pongtharangkul, T., Chuekitkumchorn, P., Suwanampa, N., Payongsri, P., Honda, K., and Panbangred, W. (2015). Kinetic properties and stability of glucose dehydrogenase from *Bacillus amyloliquefaciens* SB5 and its potential for cofactor regeneration. *AMB Express*, *5*, 68.

Singh, M., Yadav, A., Ma, X., and Amoah, E. (2010). Plasmid DNA transformation in *Escherichia Coli*: Effect of heat shock temperature, duration, and cold incubation of $CaCl_2$ treated cells. *International Journal of Biotechnology & Biochemistry*, *6*, 561–568.

CHAPTER IV
RESULTS AND DISCUSSION

4.1 The reduction of T6 and T8 catalyzed by YahK

Medium-chain fatty alcohols (C6-C12) have a wide range of applications in chemical industries, such acting as plasticizers, surfactants, and diesel-like biofuels (Ashok *et al*., 2019; Hernández Lozada *et al*., 2020; Sheng *et al*., 2016). Fatty aldehyde reductases (FALRs) catalyze the reduction of fatty aldehyde to generate the corresponding fatty alcohol. YahK, one of the FALRs, exhibits suitable activities toward medium-chain fatty aldehydes such as hexanal (**A6**) and octanal (**A8**) (Pick *et al*., 2013; Rodriguez and Atsumi, 2014). The standard protocol using UV-vis spectroscopy to characterize FALR is to monitor NADPH consumption at 340 nm, which is unsuitable for high-throughput screening (HTS) in crude lysate experiments (Mayer and Arnold, 2002). Therefore, this study sought to develop a colorimetric assay for screening YahK variants by designing medium-chain fatty aldehyde surrogates containing the formyl thioester group: the hexanal surrogate **T6** and octanal surrogate **T8**, which were proposed to be reduced by YahK. To test this proposal, the NADPH consumption catalyzed by YahK was monitored at 340 nm using UV-vis spectroscopy showing that the full reactions provided NADPH consumption compared to the control reactions without **T6** (Figure 4.1a) or **T8** (Figure 4.1b). Although YahK-catalyzed reaction of T6 or T8 were slower than its native substrates hexanal (**A6**) and octanal (**A8**), the NADPH consumption rates was higher for the **T6** and **A6** than **T8** and **A8**, respectively. These results suggest that **T6** and **T8** could be used as the substrates to study YahK.

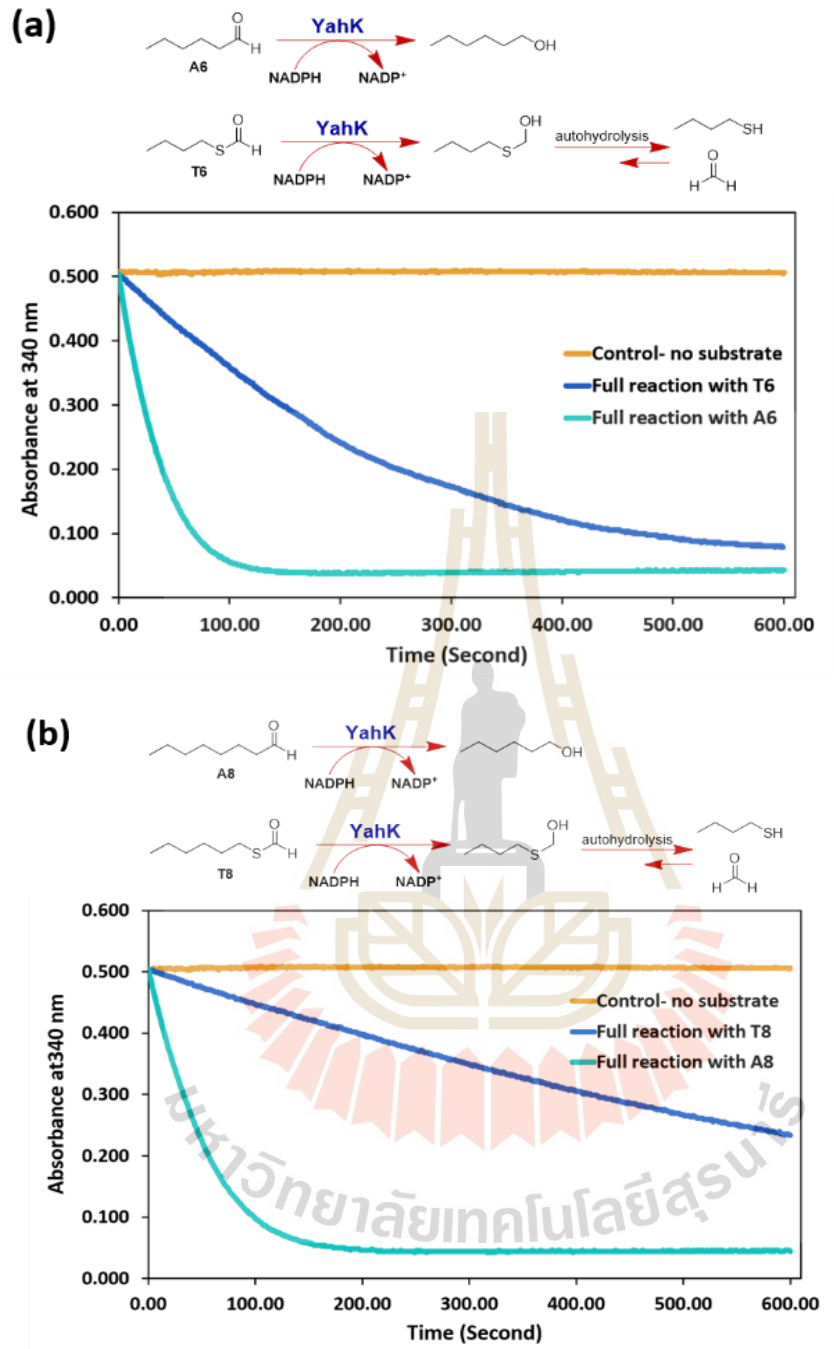

Figure 4.1 Rates of NADPH oxidation in YahK reduction of **A6**, **T6**, **A8**, and **T8**. (a) **A6**, and **T6**, (b) **A8**, and **T8** reductions catalyzed by YahK were monitored by UV spectroscopy at 340 nm. The reductions were performed with 500 μM substrate, 100 μM NADPH, 100 mM potassium phosphate buffer, pH 7.5, and 0.1 μM purified YahK.

Analysis of the apparent kinetic parameters of YahK for the substrates (**A6**, **T6**, **A8**, and **T8**) in the presence of 100 μM NADPH revealed that the apparent k_{cat} values for **T6** and **T8** decreased 4.3-fold and 5.5-fold and their K_m values increased 5.4-fold and 4.9-fold resulting in 24-fold and 27-fold decreases in the catalytic efficiency (k_{cat}/K_m) compared to **A6** and **A8**, respectively (Table 4.1 and Figure 4.2). The lower performance of **T6** and **T8** might be because of the size or polarity of the thioester group affecting the substrate-binding pocket of the enzyme. However, this result could turn out to be an advantage in high-throughput screening (HTS) for YahK engineering since it could reduce the number of variants with slight improvements showing nearly signals to wild type.

Table 4.1 Apparent kinetic parameters for different substrates.

Substrate	k_{cat} (s^{-1})	K_m (μM)	k_{cat}/K_m ($\mu M^{-1}/s^{-1}$)
A6	17.5 ± 0.5	13.8 ± 1.3	1.3 ± 0.2
T6	4.1 ± 0.2	74.0 ± 4.6	0.055 ± 0.007
A8	20.2 ± 0.9	5.9 ± 1.0	3.5 ± 1.0
T8	3.7 ± 0.2	28.9 ± 4.0	0.13 ± 0.05

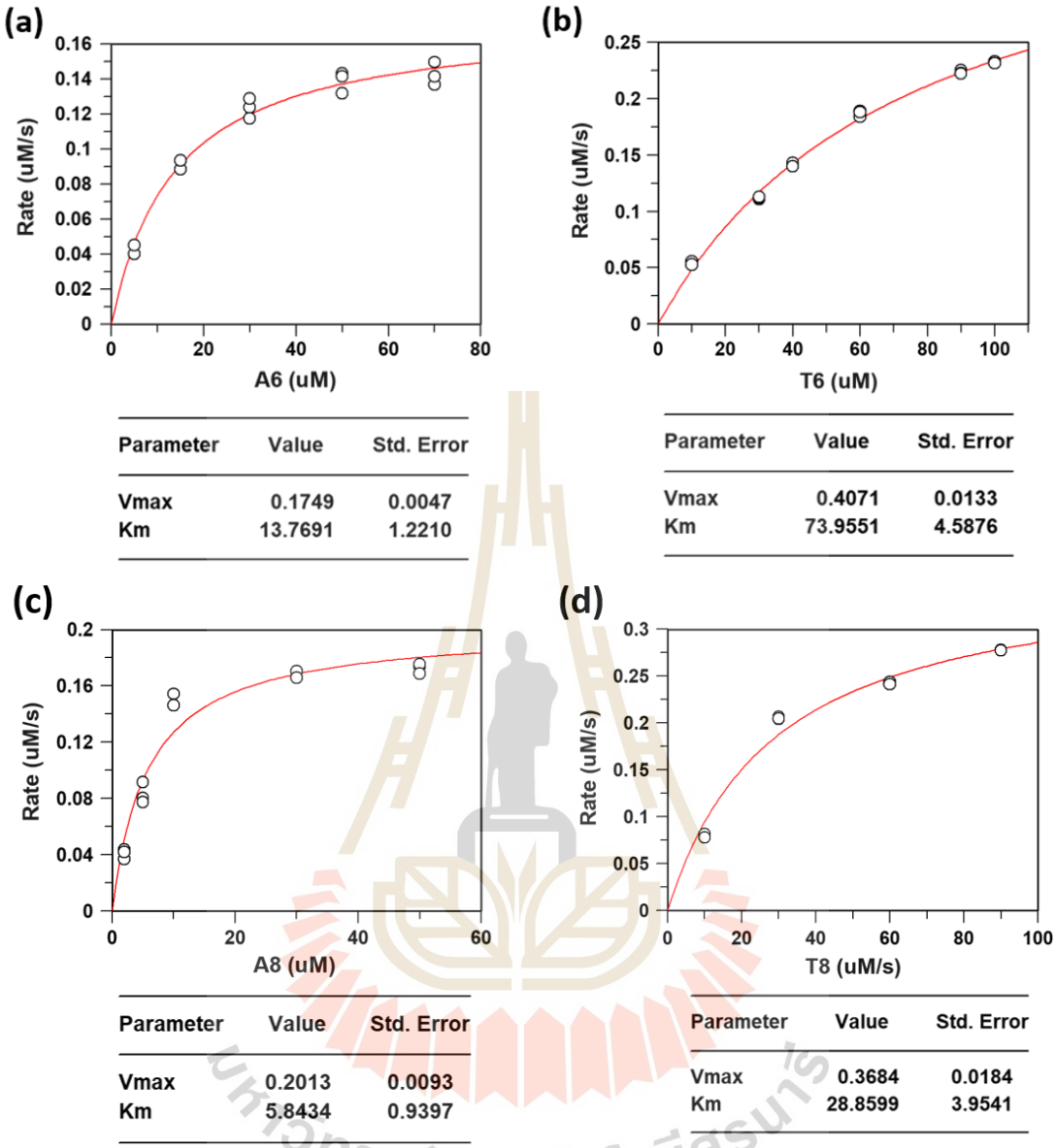

Parameter	Value	Std. Error
Vmax	0.1749	0.0047
Km	13.7691	1.2210

Parameter	Value	Std. Error
Vmax	0.4071	0.0133
Km	73.9551	4.5876

Parameter	Value	Std. Error
Vmax	0.2013	0.0093
Km	5.8434	0.9397

Parameter	Value	Std. Error
Vmax	0.3684	0.0184
Km	28.8599	3.9541

Figure 4.2 Apparent kinetic parameters for substrates with the fixed 100 μM NADPH and varied concentrations of **A6** (a), **T6** (b), **A8** (c), and **T8** (d). The reactions contained 0.1 μM purified YahK, and 100 mM potassium phosphate buffer, pH 7.5.

4.2 Investigation of formaldehyde formation from T6 and T8 reduction catalyzed by YahK

After I confirmed that **T6** and **T8** could be used as the substrates of YahK, I moved forward to investigate whether formaldehyde is formed from **T6** and **T8** reduction catalyzed by YahK (Figure 4.3). Purpald reagent is widely used for formaldehyde analysis due to its high sensitivity to formaldehyde, and it gives chromogens (purple product) after reacting with formaldehyde (Jendral *et al*., 2011; Lee and Frasch, 2001; Quesenberry and Lee, 1996; Yang *et al*., 2015). Therefore, the Purpald assay was chosen for detecting formaldehyde generated from YahK-catalyzed reactions. The Purpald solution was added to the assay after **T6** or **T8** reduction catalyzed by YahK. After derivatizing, the solution turned to purple and the formed purple product was further quantified at 550 nm in a plate reader with a formaldehyde standard calibration curve (Figure 4.4). The amounts of generated formaldehyde were nearly stoichiometric with the amount of NADPH consumption when purified YahK (Figure 4.5) and lysate containing overexpressed YahK were used (Figure 4.6) for both **T6** and **T8** substrates. These results suggest that the formyl thioester group of **T6** and **T8** could be reduced by YahK to generate formaldehyde, which could be derivatized by Purpald to yield the purple adduct, which could be visualized by naked eye or quantified at 550 nm.

Furthermore, 1-butanethiol or 1-hexanethiol was also generated from **T6** and **T8** reduction catalyzed by YahK, respectively, and they could be quantified by reacting with DTNB (5,5'-Dithiobis-(2-Nitrobenzoic Acid)) to form a yellow product, which was measured at 412 nm and compared with the calibration curve of 1-butanethiol or 1-hexanethiol (Figure 4.7 and Figure 4.8). Using purified YahK exhibited that the amount of 1-butanethiol was approximately stoichiometric with that of NADPH consumption (Figure 4.5a) while the quantity of 1-hexanethiol was slightly lower than that of NADPH consumption (Figure 4.5b). When using lysate containing overexpressed YahK, however, the amount of 1-butanethiol formation was much higher than that of NADPH consumption for **T6,** whereas the NADPH consumption (Figure 4.6a) was higher compared to the one of 1-hexanethiol formation (Figure 4.6b) for **T8** substrate. In addition, it is

important to note that the YahK-catalyzed reaction with lysate of *E. coli* containing an empty plasmid turned yellow after adding DTNB (Figure 4.6). These results suggest that cell lysates contain thiol groups (Hatahet *et al*., 2010). To avoid cellular thiol background, a DTNB assay was not chosen for detecting thiol formation from fatty aldehyde surrogate reduction catalyzed by YahK.

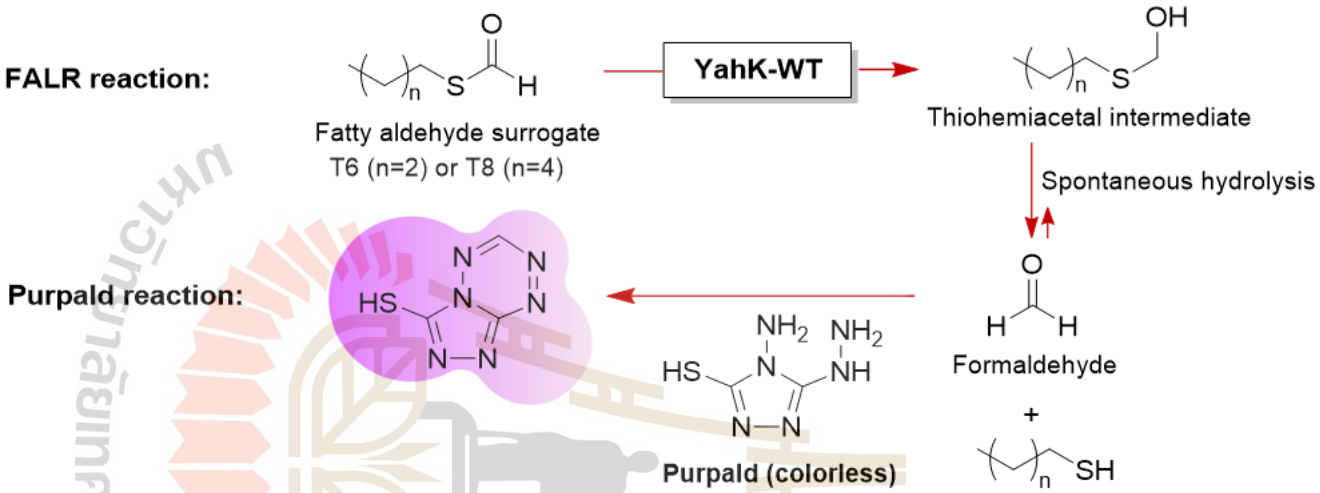

Figure 4.3 The colorimetric assay design for FALR-catalyzed reaction. The surrogate **T6** or **T8** could be reduced by YahK to generate formaldehyde via a thiohemiacetal intermediate. The generated formaldehyde could be derivatized by Purpald to yield a purple product

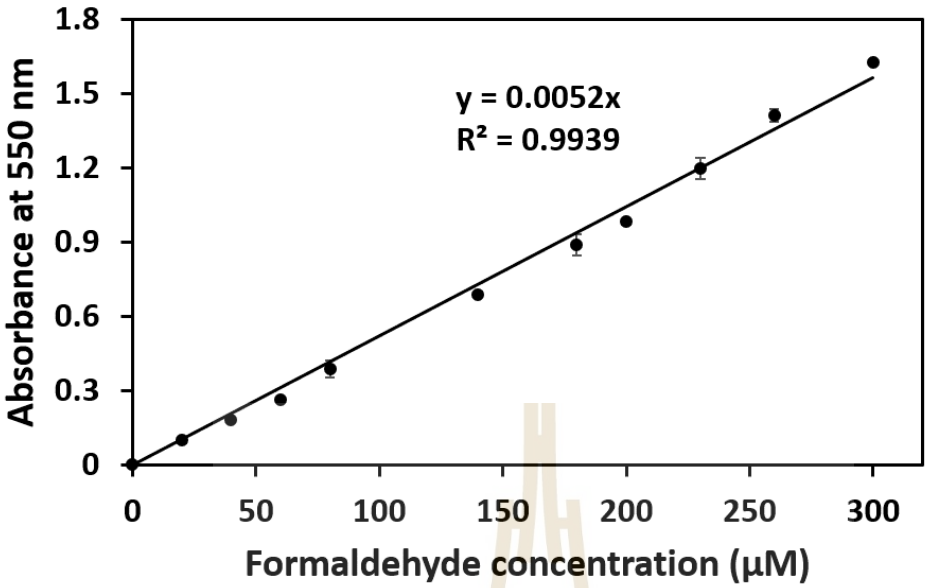

Figure 4.4 The calibration curve of formaldehyde standard solutions derivatized by the Purpald assay, in which absorption was recorded at 550 nm.

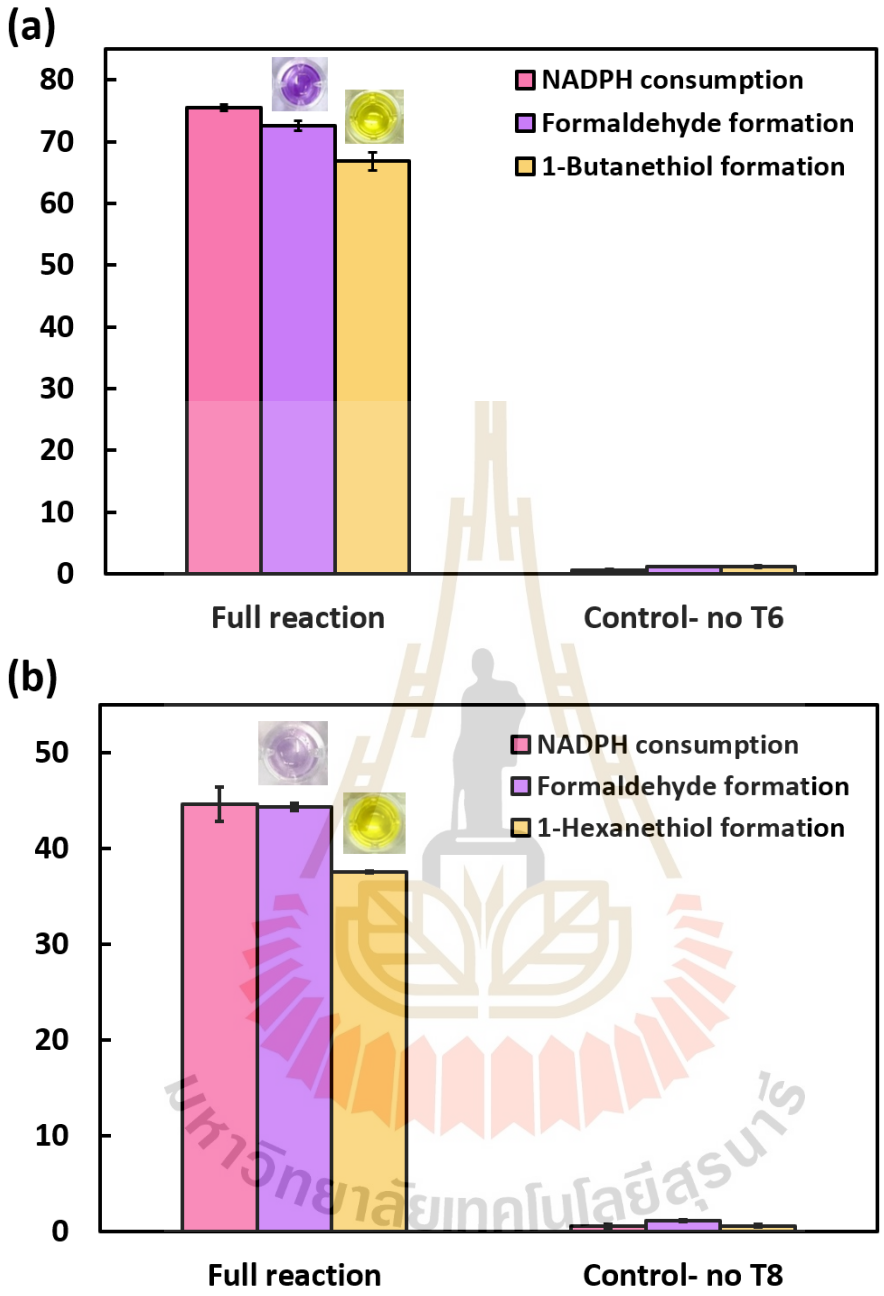

Figure 4.5

The reduction of **T6** and **T8** catalyzed by purified YahK to generate formaldehyde and thiol, which are detected by the Purpald assay and the DTNB assay, respectively. The reaction contained 500 μM **T6** (a) or **T8** (b), 0.1 μM purified YahK, 100 μM NADPH, and 100 mM potassium phosphate buffer, pH 7.5.

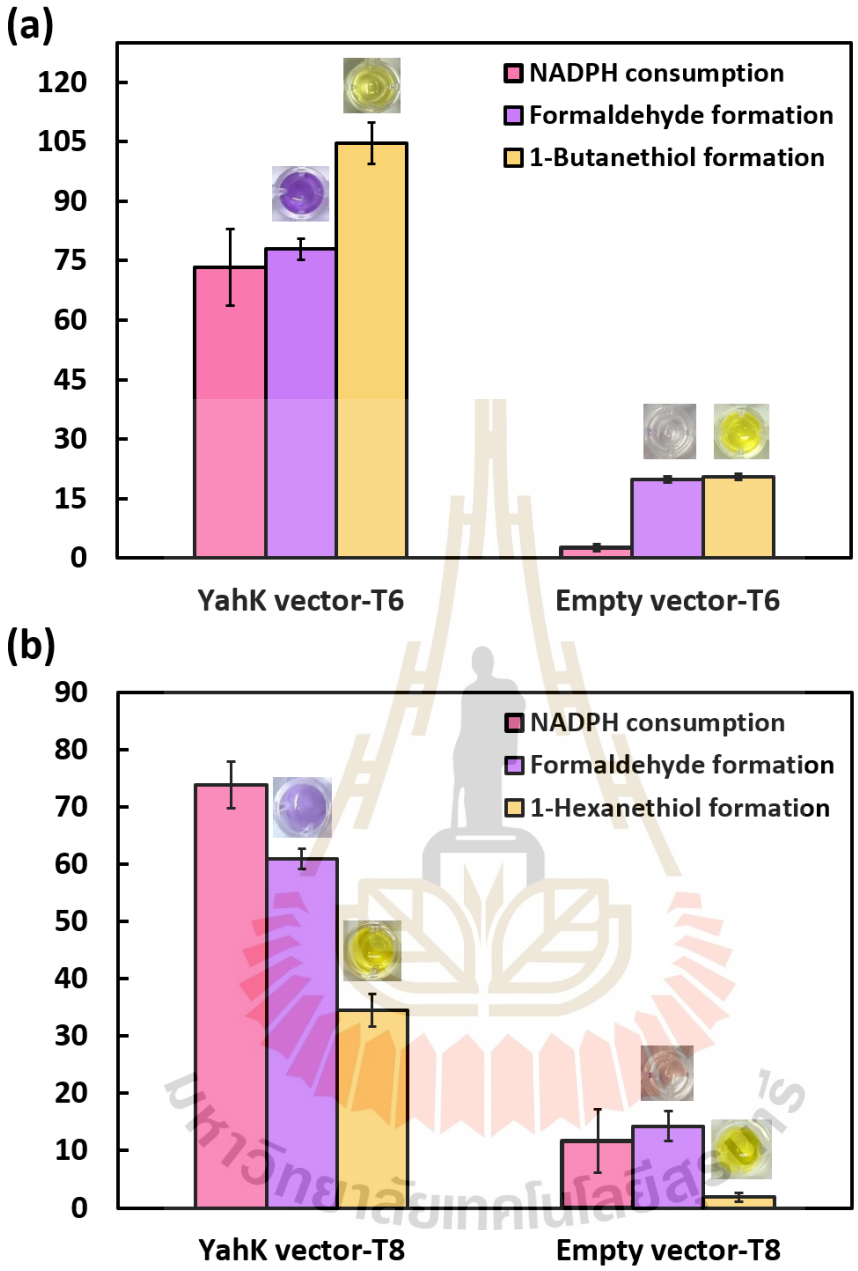

Figure 4.6 The reduction of **T6** and **T8** catalyzed by YahK in cell lysate to generate formaldehyde and thiol, which are detected by the Purpald assay and the DTNB assay, respectively. Cell lysate containing overexpressed YahK was added into the reduction mixture containing 500 μM **T6** (a) or **T8** (b), 100 μM NADPH, and 100 mM potassium phosphate buffer, pH 7.5.

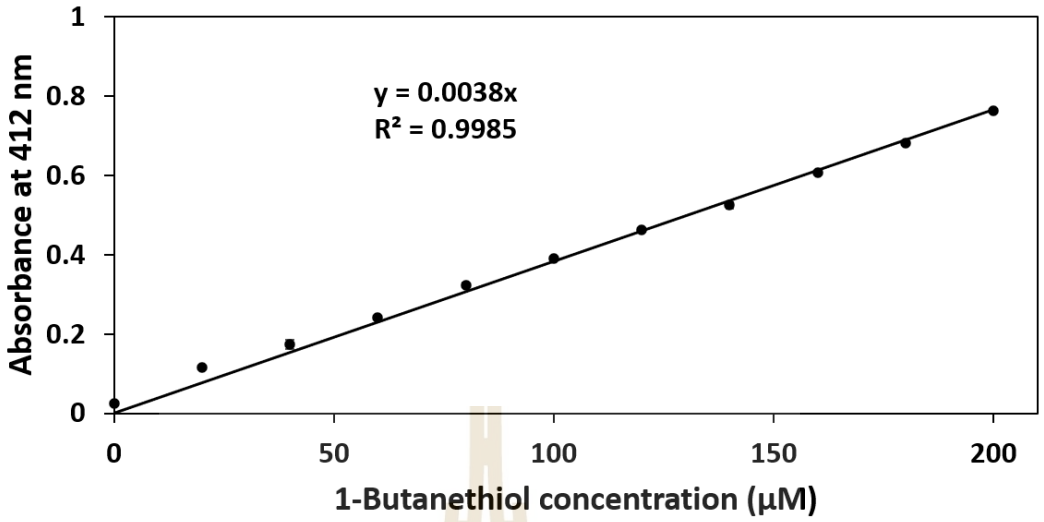

Figure 4.7 The calibration curve of 1-butanethiol standard solutions determined by the DTNB assay.

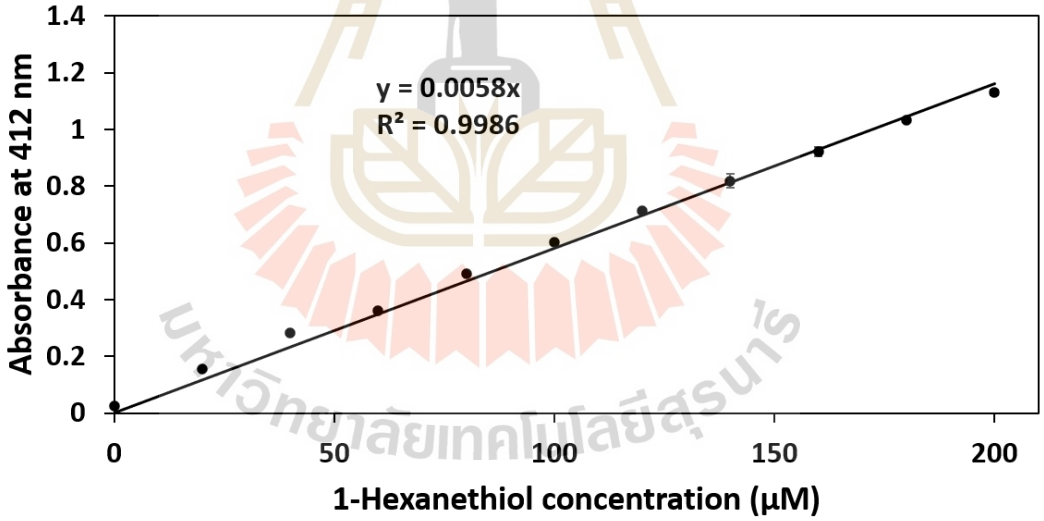

Figure 4.8 The calibration curve of 1-hexanethiol standard solutions determined by the DTNB assay.

4.3 Incorporating coenzyme regeneration system into YahK-catalyzed reaction

To demonstrate the feasibility of fatty aldehyde surrogate **T6** in high-throughput screening, this work was aimed to engineer the coenzyme specificity of YahK to enhance NADH preference. In industrial processes, NADH is preferred over NADPH because NADPH is less stable and seven times more expensive than NADH ($168/100 mg for NADPH and $25/100 mg for NADH (TCI Chemicals)). Furthermore, YahK fatty aldehyde reductase uses strictly NADPH as a coenzyme (Pick *et al*., 2013; Rodriguez and Atsumi, 2014), creating a vast challenge for using YahK in large-scale biosynthetic reaction. Therefore, this study sought to engineer the coenzyme preference of YahK by screening YahK variants with improved NADH preference.

Although NADH is cheaper than NADPH, using the reduced coenzyme NADH in the stoichiometric amount is still costly. NADH regeneration, therefore, could be a solution. (Johannes *et al*., 2007). Glucose dehydrogenase from *Bacillus amyloliquefaciens* SB5 (*Ba*GDH), which efficiently catalyzes the oxidation of β-D-glucose concomitant with the reduction of coenzyme $NAD(P)^+$ was incorporated into the assay to regenerate NAD(P)H. To avoid endogenous reductase interference, YahK-WT was expressed in *E. coli* MG1655 RARE, in which several aldehyde reductase genes were deleted. Purified *Ba*GDH was added into the lysates with the addition of 500 μM **T6**, 10 mM β-D-glucose, and 10 μM $NADP^+$. After 10 min, the Purpald solution was added to quench the reaction. The result exhibited that the reaction mixture turned purple (Figure 4.9), suggesting that *Ba*GDH can regenerate NADPH in the assay. Although wild-type YahK is strongly NADPH-dependent, it can oxidize NADH with low activity (Figure 4.10). This work, thus, tested the assay with NAD^+ added instead of $NADP^+$ showing that the reaction turned to a very light purple (Figure 4.11), probably because cell lysate contains the cellular reducing powers and *Ba*GDH can reduce both NAD^+ and $NADP^+$. This could provide high background in the screening.

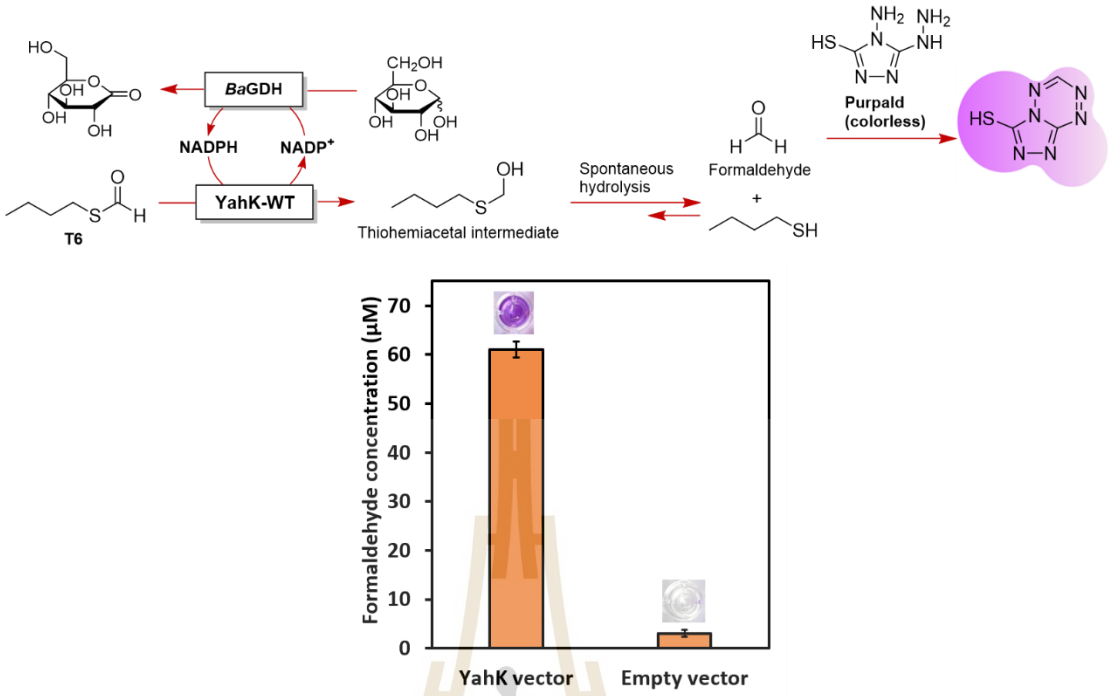

Figure 4.9 Coenzyme regeneration tested by coupling *Ba*GDH with the YahK-WT reaction. The reaction was performed by adding 500 μM **T6**, 10 μM $NADP^+$, and 2 μM purified *Ba*GDH into the lysate.

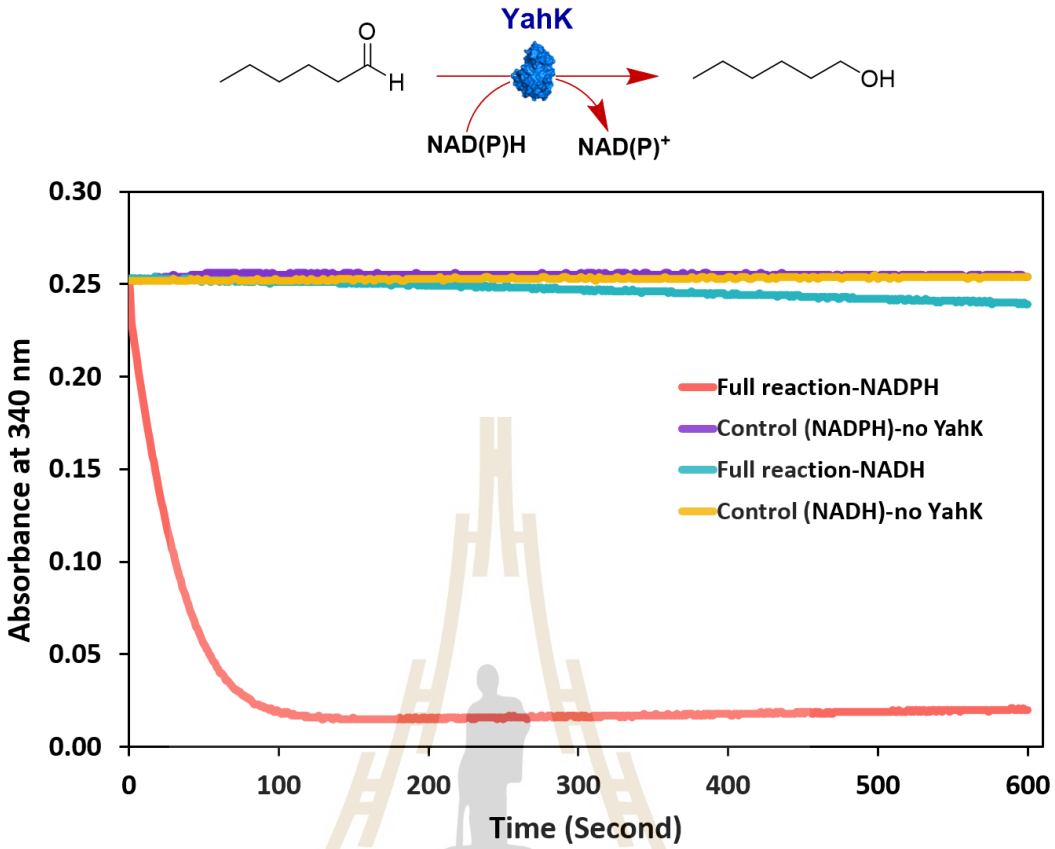

Figure 4.10 YahK-catalyzed reaction with NADH or NADPH. The reductions were performed with 500 μM **A6**, 100 μM NADPH or NADH, 100 mM potassium phosphate buffer, pH 7.5, and 0.1 μM purified YahK.

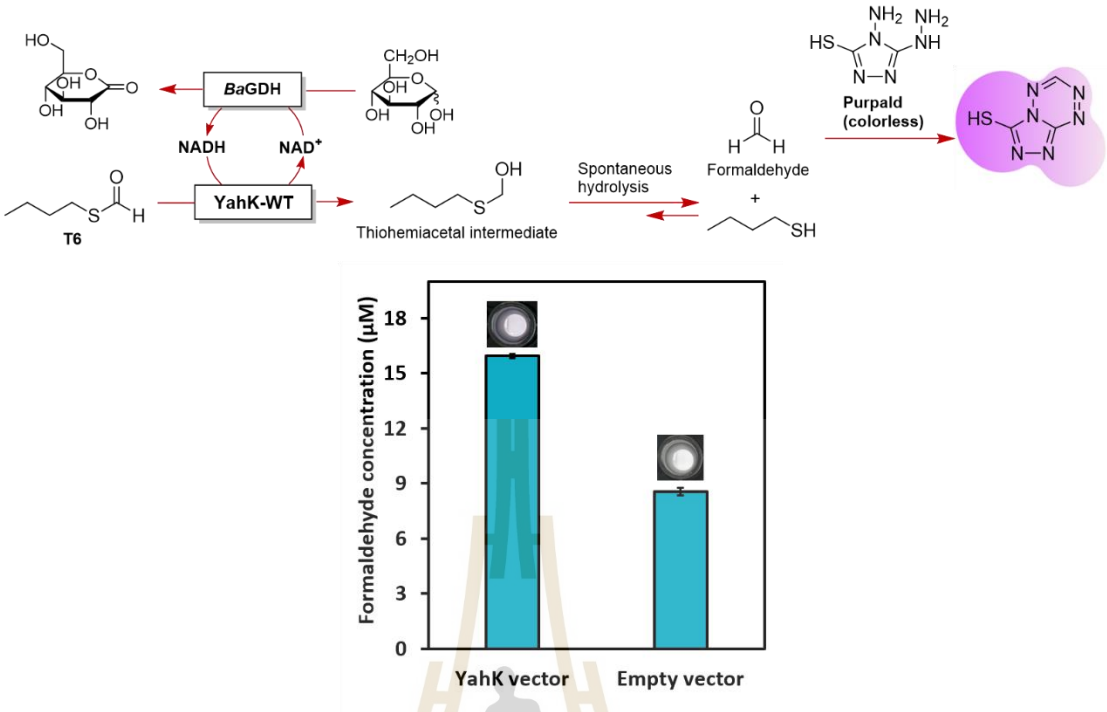

Figure 4.11 Coenzyme regeneration by *Ba*GDH tested by coupling with the YahK-WT reaction. The reaction was performed by adding 500 μM **T6**, 10 μM NAD^+, and 2 μM purified *Ba*GDH into the lysate.

To avoid signals from NADPH-or NADH-dependent reactions, I incorporate *Pseudomonas* sp. 101 formate dehydrogenase (*Pa*FDH-WT) into the assay, as it is highly specific for NAD^+. *Pa*FDH-V9, which is its variant and preferentially reduces $NADP^+$, was used for comparison to test this hypothesis. Purified *Pa*FDH-WT or *Pa*FDH-V9 was added into the lysates with 500 μM **T6**, 10 mM formate, and 10 μM $NADP^+$. After 10 min, the reaction was derivatized by adding Purpald solution showing that only the reaction with *Pa*FDH-V9 turned purple (Figure 4.12) since it regenerated NADPH in the assay. In addition, another assay was set by adding purified *Pa*FDH-WT into the lysate containing 500 μM **T6**, 10 mM formate, and 10 μM NAD^+. After quenching the reaction with Purpald solution, the assay did not turn purple at all (Figure 4.13). This suggests that *Pa*FDH-WT strictly uses NAD^+ with simultaneous oxidation of formate. Therefore,

*Pa*FDH-WT is suitable to incorporate into the YahK-catalyzed reaction to regenerate NADH for coenzyme specificity engineering of YahK variants to increase NADH activity.

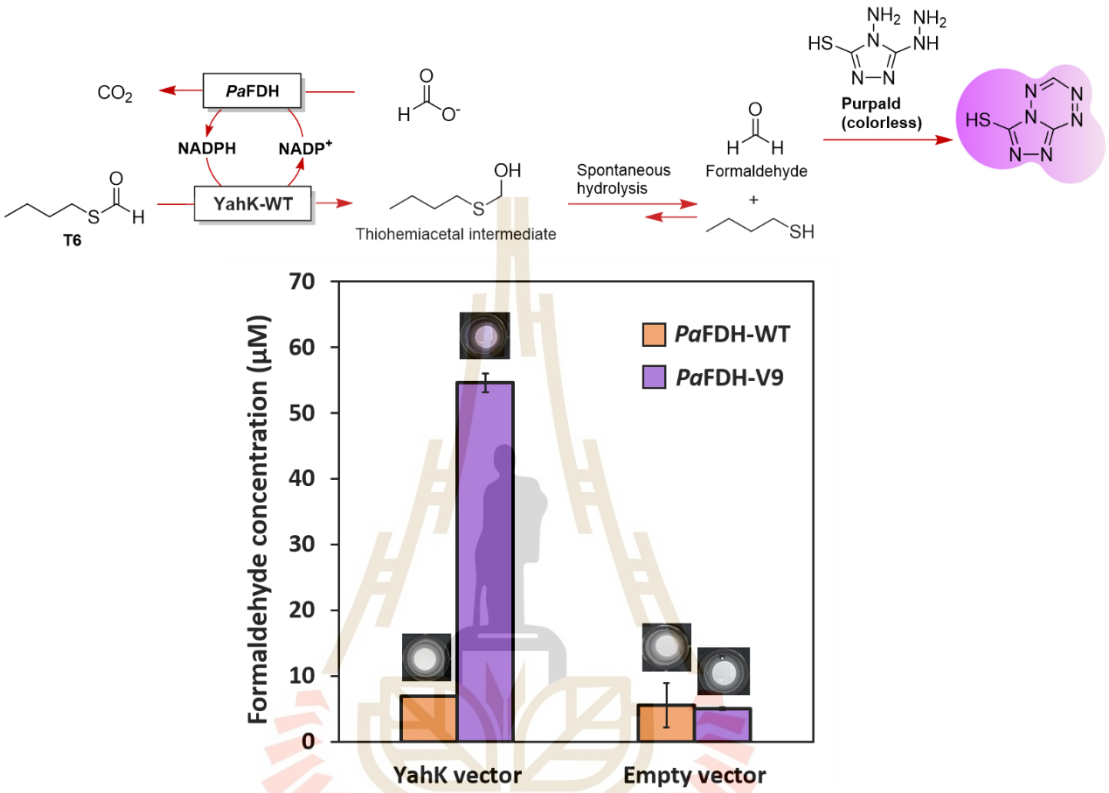

Figure 4.12 Coenzyme regeneration by *Pa*FDH-WT or *Pa*FDH-V9 teste by coupling with YahK-WT reaction. The reaction was performed by adding 500 μM **T6**, 10 μM $NADP^+$, and 2 μM purified *Pa*FDH-WT or *Pa*FDH-V9 into the lysate.

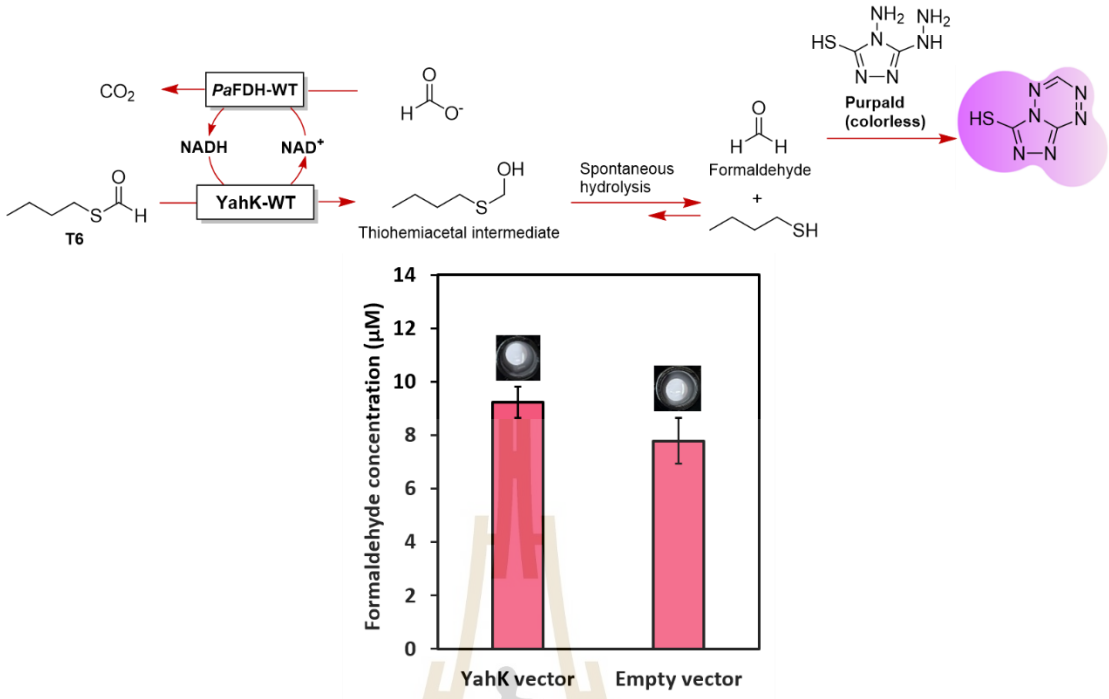

Figure 4.13 Coenzyme regeneration by *Pa*FDH-WT tested by coupling with the YahK-WT reaction. The reaction was performed by adding 500 μM **T6**, 10 μM NAD^+, and 2 μM purified *Pa*FDH-WT into the lysate.

4.4 Using the surrogate T6 in high-throughput screening of YahK engineering

In the workflow of high-throughput screening for coenzyme engineering of YahK (Figure 4.14), NADPH was docked into the coenzyme binding site of YahK wild-type (PDB: 1UUF), showing that T205 and T206 have hydrogen bonds to the phosphate group of NADPH (Figure 4.15). I, therefore, incorporated NNK degenerate codons at these two sites to yield a mutant library, which its size was estimated to be 1×10^3 independent transformants. The library was transformed into MG1655 RARE and each resulting colony was cultured in 96-well plates for YahK variant expression. After centrifugation, the cells were lysed with lysozyme at 37°C for 30 min. The master mix containing 500 μM **T6**, 10 mM formate, 5 μM *Pa*FDH-WT, and 10 μM NAD^+ was added to the cell lysate. After 10 min of FALR-catalyzed reaction, the Purpald solution was then added to quench the reaction and derivatize the generated formaldehyde. MG1655 RARE harboring wild-type YahK served as a negative control. Numerous positive hits were observed through naked eyes. I further identified the two best variants, E3 and C8, based on the absorbance at 550 nm. Sequencing the two variants revealed that the E3 contains T206V and the C8 contains T205S-T206M.

I determined the apparent kinetic parameters of two YahK variants for NADH and NADPH (Table 4.2, Figure 4.16). Compared to WT, E3 and C8 exhibited ~4.5- and ~6.4-fold relative coenzyme specificity switches from NADPH to NADH, respectively, based on specificity constant. The mutations of E3 and C8 destabilized binding with 2-phosphate of NADPH due to the hydrophobic residues. These results demonstrated the successful application of surrogate **T6** in high-throughput screening to identify YahK variants with improved NADH activity from a diverse mutant library.

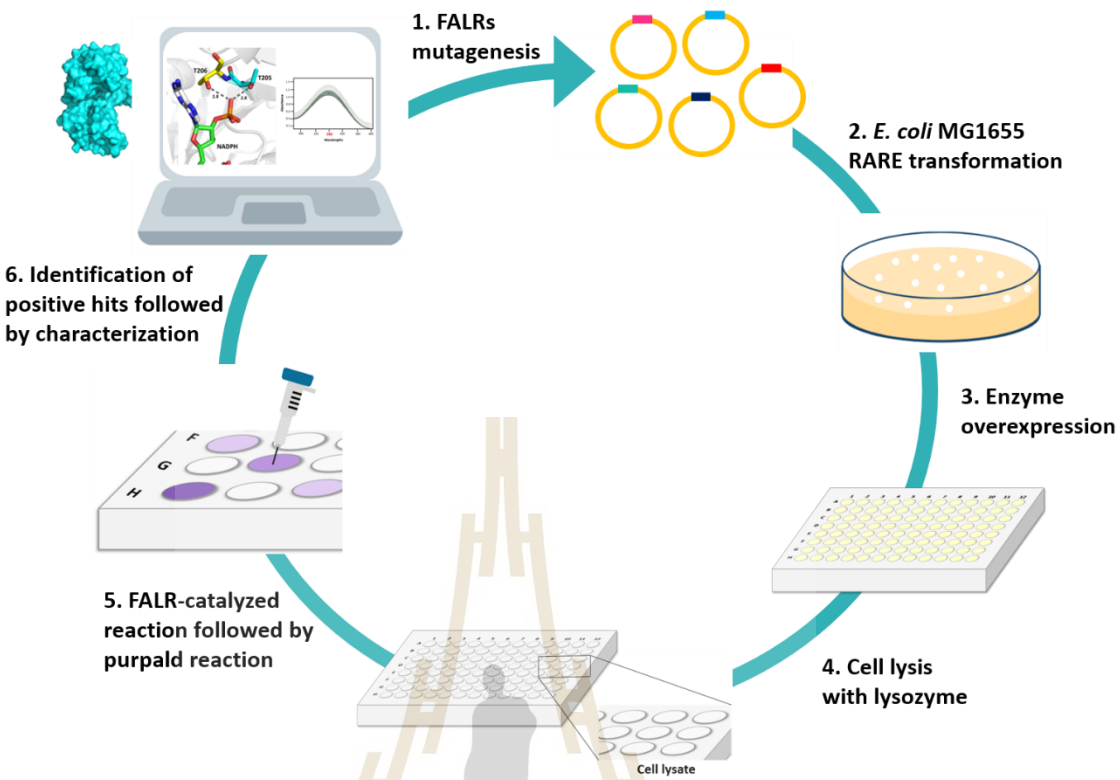

Figure 4.14 Schematic workflow overview for coenzyme preference engineering of FALR.

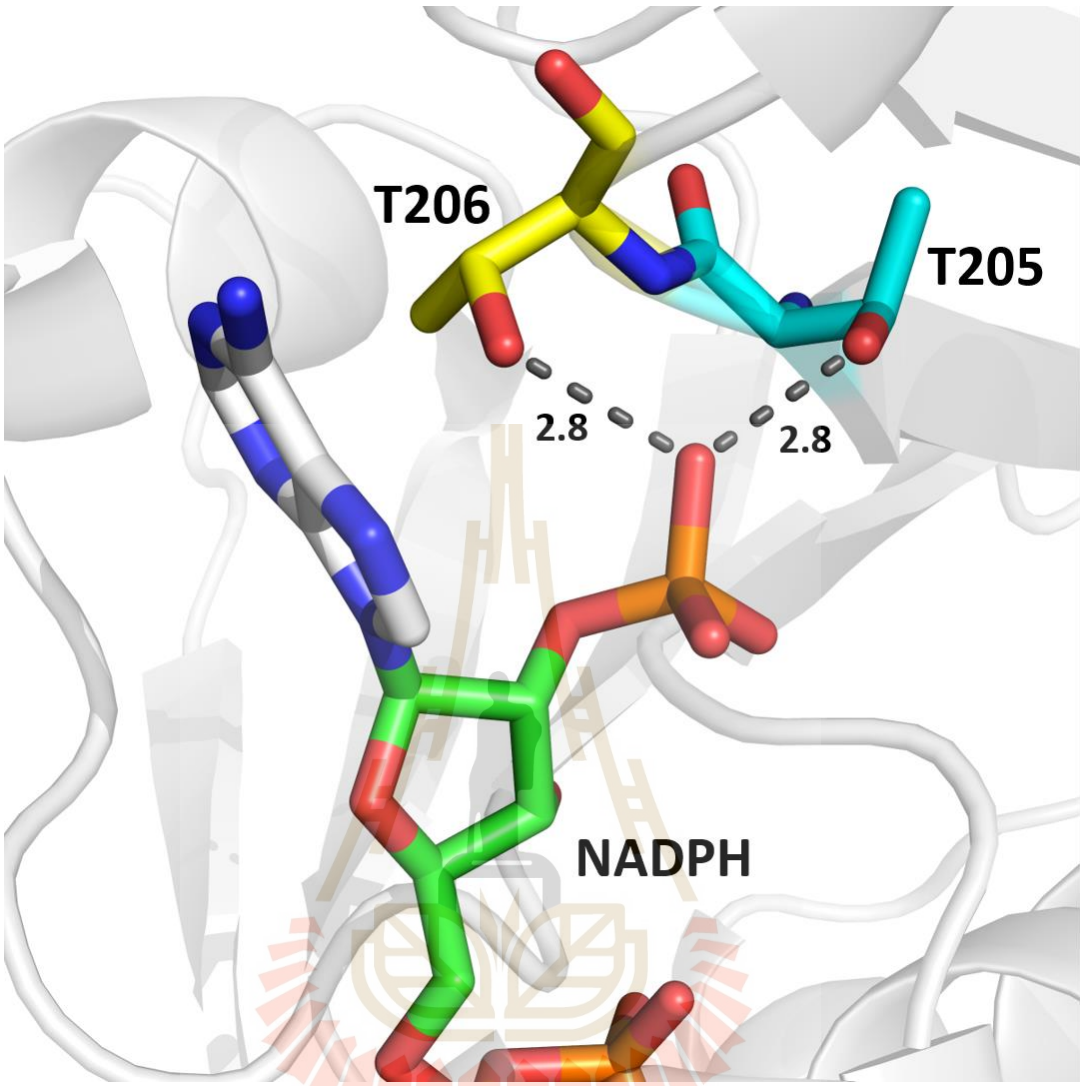

Figure 4.15 Docking NADPH in the coenzyme binding site of YahK showed that T205 and T206 have hydrogen bonding interactions with the 2'phosphate group of NADPH.

Table 4.2 Apparent kinetic parameter for NADH and NADPH.

NADH			
Variant	k_{cat} (s^{-1})	K_m (μM)	k_{cat}/K_m ($\mu M^{-1}/s^{-1}$)
WT	1.63 ± 0.12	245 ± 31	0.0067 ± 0.0018
E3 (T206V)	3.77 ± 0.20	245 ± 23	0.0150 ± 0.0028
C8 (T205S-T206M)	2.05 ± 0.16	276 ± 41	0.0074 ± 0.0017
NADPH			
Variant	k_{cat} (s^{-1})	K_m (μM)	k_{cat}/K_m ($\mu M^{-1}/s^{-1}$)
WT	44.5 ± 1.4	12.5 ±1.8	3.56 ± 0.62
E3 (T206V)	116.6 ± 2.4	66.1 ± 4.0	1.77 ± 0.14
C8 (T205S-T206M)	73.4 ± 3.3	121 ± 13	0.61 ± 0.09

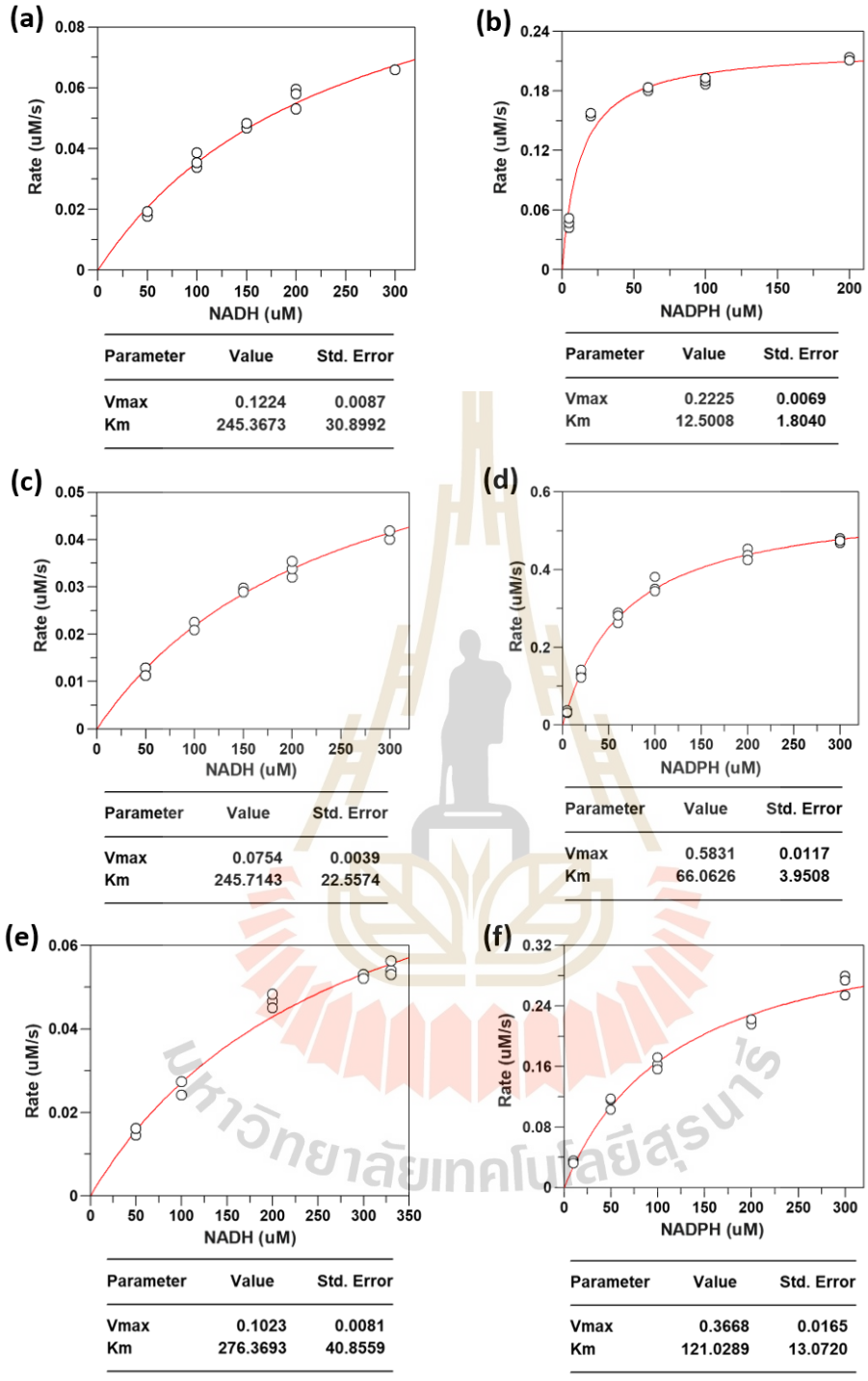

Figure 4.16 Apparent kinetic parameters of YahK (a and b), E3 (c and d), and C8 (e and f) for NADH and NADPH. Reactions were performed with varied concentrations of NADH and NADPH, 0.1 μM purified YahK, 500 μM **A6**, and 100 mM potassium phosphate buffer, pH 7.5.

4.5 References

Ashok, B., Nanthagopal, K., Darla, S., Chyuan, O. H., Ramesh, A., Jacob, A., Sahil, G., Thiyagarajan, S., and Geo, V. E. (2019). Comparative assessment of hexanol and decanol as oxygenated additives with calophyllum inophyllum biodiesel. *Energy*, *173*, 494–510.

Hatahet, F., Nguyen, V. D., Salo, K. E., and Ruddock, L. W. (2010). Disruption of reducing pathways is not essential for efficient disulfide bond formation in the cytoplasm of *E. coli*. *Microbial Cell Factories*, *9*(1), 67.

Hernández Lozada, N. J., Simmons, T. R., Xu, K., Jindra, M. A., and Pfleger, B. F. (2020). Production of 1-octanol in *Escherichia coli* by a high flux thioesterase route. *Metabolic Engineering*, *61*, 352–359.

Jendral, J. A., Monakhova, Y. B., and Lachenmeier, D. W. (2011). Formaldehyde in Alcoholic Beverages: Large Chemical Survey Using Purpald Screening Followed by Chromotropic Acid Spectrophotometry with Multivariate Curve Resolution. *International Journal of Analytical Chemistry*, *2011*, 797604.

Johannes, T. W., Woodyer, R. D., and Zhao, H. (2007). Efficient regeneration of NADPH using an engineered phosphite dehydrogenase. *Biotechnology and Bioengineering*, *96*(1), 18–26.

Lee, C.-H., and Frasch, C. E. (2001). Quantification of Bacterial Polysaccharides by the Purpald Assay: Measurement of Periodate-Generated Formaldehyde from Glycol in the Repeating Unit. *Analytical Biochemistry*, *296*(1), 73–82.

Mayer, K. M., and Arnold, F. H. (2002). A Colorimetric Assay to Quantify Dehydrogenase Activity in Crude Cell Lysates. *SLAS Discovery*, *7*(2), 135–140.

Pick, A., Rühmann, B., Schmid, J., and Sieber, V. (2013). Novel CAD-like enzymes from *Escherichia coli* K-12 as additional tools in chemical production. *Applied Microbiology and Biotechnology*, *97*(13), 5815–5824.

Quesenberry, M. S., and Lee, Y. C. (1996). A Rapid Formaldehyde Assay Using Purpald Reagent: Application under Periodation Conditions. *Analytical Biochemistry*, *234*(1), 50–55.

Rodriguez, G. M., and Atsumi, S. (2014). Toward aldehyde and alkane production by removing aldehyde reductase activity in *Escherichia coli*. *Metabolic Engineering*, *25*, 227–237.

Sheng, J., Stevens, J., and Feng, X. (2016). Pathway Compartmentalization in Peroxisome of *Saccharomyces cerevisiae* to Produce Versatile Medium Chain Fatty Alcohols. *Scientific Reports*, *6*(1), 26884.

Yang, Y., Chi, Y. T., Toh, H. H., and Li, Z. (2015). Evolving P450pyr monooxygenase for highly regioselective terminal hydroxylation of n-butanol to 1,4-butanediol. *Chemical Communications*, *51*(5), 914–917.

CHAPTER V
CONCLUSIONS

To sum up, this study was to develop the assay using fatty aldehyde surrogates for high-throughput screening (HTS) of fatty alcohol reductase (FALR). The surrogates containing the formyl thioester group could be reduced by FALR to generate formaldehyde via thiohemiacetal intermediate. The resulting formaldehyde could simply be derivatized by Purpald to yield the purple product, which is visualized by the naked eye and quantified by UV-Vis spectroscopy at 550 nm. Furthermore, this work successfully demonstrated the capability of the surrogate **T6** in HTS of FALR with increased NADH preference. I identified the two best variants: E3 (T206V) and C8 (T205ST206M). C8 showed a ~6.4-fold relative coenzyme specificity switch from NADPH to NADH while E8 exhibited a ~4.5-fold relative coenzyme specificity switch. In HTS, the coenzyme regeneration system using *Pa*FDH-WT was incorporated into the assay to regenerate NADH. In addition, I envision the surrogate could further be used to engineer other fatty aldehyde reductases for specific purposes and the formyl thioester group could also be applied in other surrogate designs for HTS of other reductases engineering.

APPENDICES

APPENDIX A

YAHK PURIFICATION AND NNK LIBRARY CLONING

A.1 YahK Purification

After protein expression, the cells were harvested and then lysed by sonication, followed by centrifugation to obtain the supernatant. The resulting supernatants were loaded onto the Ni-NTA column (QIAGEN) and the proteins were eluted by increasing imidazole concentration. The pure proteins were checked by SDS PAGE **(Figure A1).** The molecular weight of YahK is 40.3 kDa, which is consistent with SDS PAGE analysis.

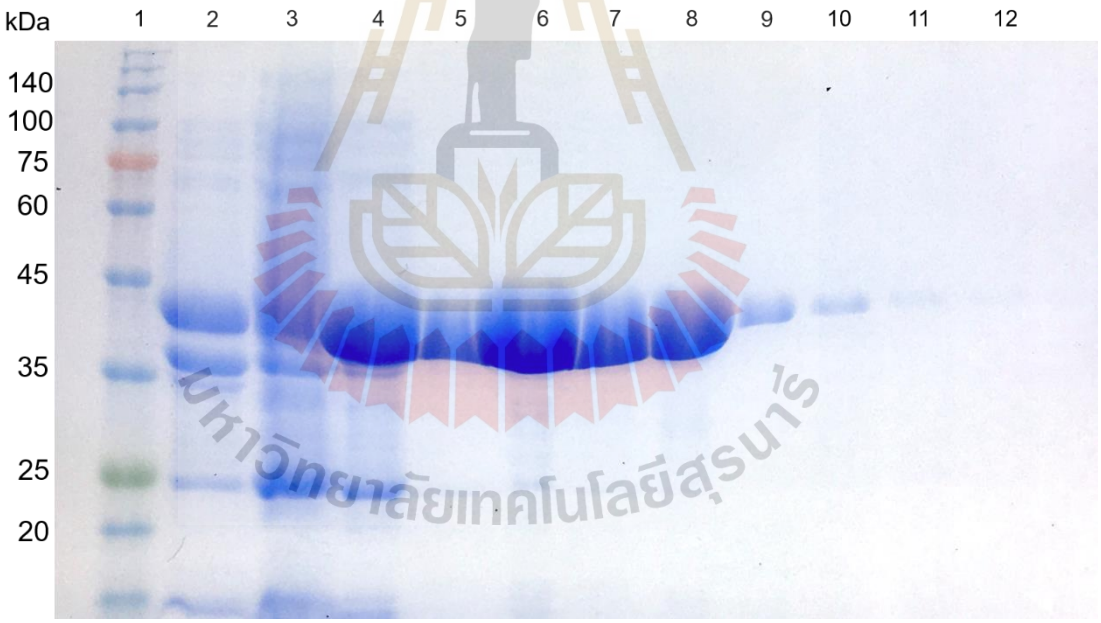

Figure A.1 The SDS-PAGE analysis of YahK. Lane 1: marker; Lane 2: pellet; Lane 3: flow-through; Lane 4 and 5: elution with 20 mM imidazole; Lane 6 and 7: elution with 50 mM imidazole; Lane 8 and 9: elution with 100 mM imidazole; Lane 10 and 11: elution with 150 mM imidazole; Lane 12: elution with 250 mM imidazole.

A.2 Cloning of NNK library

The target DNA band was separated on agarose gel electrophoresis after amplifying two-site saturation mutagenesis library T205/T206 from pET30a-*EcYahK* using pair of degenerate primers RYL185/RYL186. The expected size of target PCR product is about 7,114 bp (Figure A2).

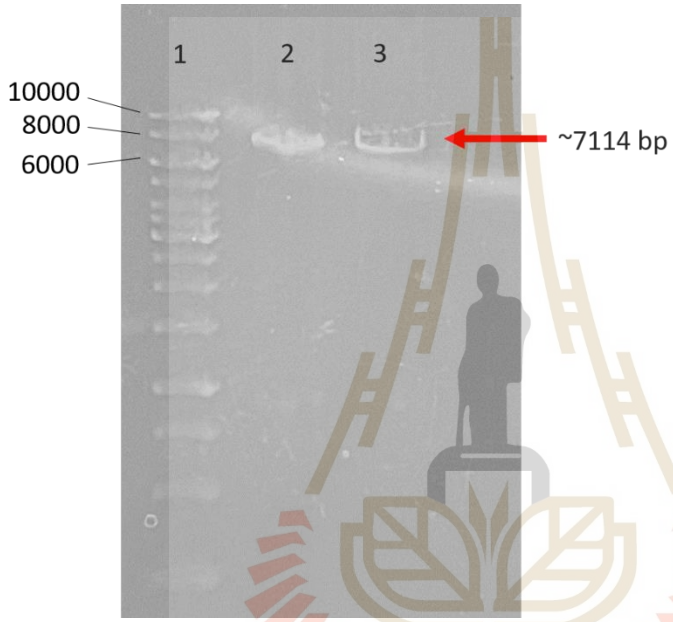

Figure A.2 Agarose gel electrophoresis of NNK library. Lane 1: Marker; Lane 2 PCR product; Lane 3 PCR product amplified in GC buffer.

APPENDIX B

PUBLICATIONS AND PRESENTATIONS

B.1 List of publications

Ngivprom, U., Lasin, P., Khunnonkwao, P., Worakaensai, S., Jantama, K., Kamkaew, A., Lai, R-Y. (2022). Synthesis of nicotinamide mononucleotide from xylose via coupling engineered *Escherichia coli* and a biocatalytic cascade. *ChemBioChem, 23,* e202200071.

Worakaensai, S., Kluaiphanngam, S., Wet-osot, S., Charoenwattanasatien, R., Ngivprom, U., Duangkamol, C., Kamkaew, A., Lai, R-Y. (2021). Design of a surrogate for high throughput screening of fatty aldehyde reductase engineering. *Chem Comm*, *57,* 13373-13376.

Wangngae, S., Pewklang T., Chansaenpak, K., Ganta, P., Worakaensai, S., Siwawannapong, K., Kluaiphanngam, S., Nantapong, N., Lai, R-Y., Kamkaew, A. (2021). A chalcone-based fluorescent responsive probe for selective detection of nitroreductase activity in bacteria. *New J. Chem, 45,* 11566-11573.

B.2 List of poster presentation

Suphanida Worakaensai, Surayut Kluaiphanngam, Sirawit Wet-Osot, Utumporn Ngivprom, Anyanee Kamkaew, and Rung Yi Lai. (November 2020). The surrogate design for high-throughput screening of fatty aldehyde reductases. **The 15th International Symposium of The Protein Society of Thailand**, Bangkok, Thailand.

Suphanida Worakaensai, Surayut Kluiphanngam, Sirawit Wet-Osot, Ratana Charoenwattanasatien, Utumporn Ngivprom, Anyanee Kamkaew, and Rung-Yi Lai. (November 2022). High-throughput screening using designed surrogate for fatty aldehyde reductase engineering. **The 34th Annual Meeting of the Thai Society for Biotechnology and International Conference**, Bangkok, Thailand.

Manuscript Chem Comm

(journal impact factor = 6.065)

ChemComm

ROYAL SOCIETY OF CHEMISTRY

COMMUNICATION

Cite this: *Chem. Commun.*, 2021, **57**, 13373

Received 28th September 2021,
Accepted 2nd November 2021

DOI: 10.1039/d1cc05472d

rsc.li/chemcomm

Design of a surrogate for high throughput screening of fatty aldehyde reductase engineering†

Suphanida Worakaensai,[a] Surayut Kluaiphanngam,[a] Sirawit Wet-osot,[a] Ratana Charoenwattanasatien,[bc] Utumporn Ngivprom,[a] Chuthamat Duangkamol,[a] Anyanee Kamkaew[a] and Rung-Yi Lai[*ac]

We designed and synthesized a fatty aldehyde surrogate containing a formyl thioester group, which can be reduced by fatty aldehyde reductase (FALR) with stoichiometric formaldehyde generation. It can be rapidly visualized and quantified using the Purpald assay. We demonstrated its successful application in the high throughput screening of FALR engineering.

Fatty alcohols are important oleochemicals that have been used for surfactant and detergent production in various industries.[1] Furthermore, they are also components of cosmetics, foods, and industrial solvents. Their global market size is expected to continuously grow from 5.4 billion USD in 2020 to 7.0 billion USD by 2025. Currently, fatty alcohols are mostly produced from petrochemical and plant oil feedstocks. However, petroleum supply and global warming issues have raised substantial concern and have motivated people to find sustainable solutions for their production. Metabolic engineering is an alternative strategy for the development of microbial biocatalysts by converting renewable resources such as plant biomass to fatty alcohols and their derivatives.[2–6] Several pathways have been developed to generate fatty alcohols. In all the pathways, fatty aldehydes are a common intermediate, which can be reduced by FALRs to generate fatty alcohols as the product. However, the investigation of FALRs has not attracted significant attention for further engineering. FALRs use NADPH/NADH as the cofactor to catalyze fatty aldehyde reduction. The standard protocol for the characterization involves monitoring of the consumption of NAD(P)H using UV-vis spectroscopy at 340 nm with purified enzymes or a crude lysate containing overexpressed FALRs. This protocol could also be applied in the screening or enzymatic characterization of mutants designed by rational protein engineering using site-directed mutagenesis.[7] Generally, the number of variants is less. However, in directed evolution, its library size is considerably larger. Therefore, this method cannot rapidly identify positive hits with activity measurement in high throughput screening (HTS) with good sensitivity.[8] In addition, it cannot be coupled with the NADPH/NADH regeneration system using a catalytic cofactor quantity to reduce the screening cost.[9] Hence, we sought to design a surrogate of fatty aldehyde, capable of displaying color in assays. The color could be observed using the naked eye and quantified with UV-vis spectroscopy for the identification of benign variants in a library.

To avoid the fact that FALRs cannot reduce a surrogate containing a chromophore, which might affect substrate binding, we propose a surrogate that generates a byproduct after the FALR-catalyzed reduction. The byproduct can be derivatized to generate a color adduct. Thus, we reviewed the reduction mechanism of carbonyl groups catalyzed by enzymes. Fatty acyl-CoA reductase[10] and the thioester reductase domain[11] in PKS and NRPS were considered as candidates. They use NADPH or NADH to reduce the thioester group of fatty acyl-CoA and acyl-*S*-polyketides or peptidyl-*S*-nonribosomal peptides to generate the common intermediate thiohemiacetal followed by spontaneous hydrolysis to generate aldehydes. Therefore, we designed a surrogate containing a formyl thioester group to mimic the aldehyde group (Scheme 1).

We propose a surrogate that after reduction forms a thiohemiacetal intermediate followed by spontaneous hydrolysis to generate formaldehyde as the byproduct. Formaldehyde is derivatized by the Purpald reagent to form a purple adduct. This derivatization was successfully applied in the hydroxylation activity screening of cytochrome P450 enzyme libraries;[12,13] however the surrogates generate a different intermediate, hemiacetal, to release formaldehyde after hydrolysis. To test our proposal, the hexanal surrogate **T6** and the decanal surrogate **T10** (Scheme 1) were successfully synthesized from the corresponding 1-alkanethiol

[a] *School of Chemistry, Institute of Science, Suranaree University of Technology, Nakhon Ratchasima, 30000 Thailand. E-mail: rylai@sut.ac.th*
[b] *Synchrotron Light Research Institute (Public Organization), 111 University Avenue, Nakhon Ratchasima, 30000 Thailand*
[c] *Center for Biomolecular Structure, Function and Application, Suranaree University of Technology, Nakhon Ratchasima, 30000 Thailand*

† Electronic supplementary information (ESI) available. See DOI: 10.1039/d1cc05472d

Manuscript Chem Comm

(journal impact factor = 6.065)

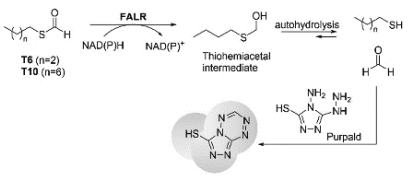

Scheme 1 The surrogate containing a formyl thioester group generates formaldehyde *via* a thiohemiacetal intermediate after the FALR-catalyzed reduction. Formaldehyde is derivatized by Purpald to form a purple adduct.

and formic acid in the presence of excess acetic anhydride (see the ESI†). As the formyl thioester group was reported to be hydrolyzed in basic or acidic buffers,[14,15] the stability of **T6** was investigated in DMSO-d_6 containing 20% of an assay buffer (100 mM potassium phosphate, pH 7.5) and analyzed using ^{1}H-NMR (Fig. S3, ESI†). We did not observe any new signals in 10 min, which is the FALR assay time. Furthermore, the DTNB assays did not detect any thiol generation in one hour (Fig. S4, ESI†). Both analyses suggest that the formyl thioester group is stable in the assay buffer.

We tested the reduction of **T6** using three in-house *Escherichia coli* FALRs (YahK, DkgA, and YbbO), that exhibit good activities towards medium-chain fatty aldehydes, such as hexanal (**A6**).[16] Furthermore, **T10** was tested for *Marinobacter aquaeolei* VT8 alcohol-forming acyl-CoA reductase (MAACR), whose preferred aldehyde is decanal (**A10**).[17] The NADPH consumption for each reductase was analyzed using UV-vis spectroscopy at 340 nm (Fig. S5a–S8a, ESI†). All the reductase assays provided the NADPH consumption in the full reactions compared with the control reactions without **T6** or **T10**. In the **T6** reduction by DkgA (Fig. S6a, ESI†) and YbbO (Fig. S7a, ESI†), enzyme concentrations of 20 μM revealed an evident NADPH consumption within the same assay time. Furthermore, YbbO exhibited better reduction activities on **A10** and **T10** than that on **A6** and **T6**. This suggests that YbbO has a preference for longer chain fatty aldehydes.[18] Although the reductases cannot reduce **T6** and **T10** to the same extent as **A6** and **A10**, the NADPH consumptions in the **T6** and **T10** reduction relatively represent those of **A6** and **A10** by the same reductases. Furthermore, NADPH and NADH cannot reduce **T6** (Fig. S9, ESI†). These results confirm that the reduction is catalyzed by the reductases. Therefore, researchers could also use a formyl thioester surrogate as the substrate to study FALRs. *E. coli* YahK (hereafter named YahK-WT) was reported to have broad activity towards medium-chain fatty aldehydes[16] and other aldehyde substrates.[19] Therefore, it represents a good NADPH dependent biocatalyst for alcohol production. Therefore, YahK was chosen for the demonstration of **T6** application. The apparent kinetic parameters of **T6** and **A6** for YahK-WT were determined in the presence of 100 μM NADPH (Table S1 and Fig. S10, ESI†). In comparison with the **A6** parameters, the k_{cat} of **T6** decreases 4.3-fold, and its K_m increases 5.4-fold. Therefore, the ratio of k_{cat}/K_m for **A6** to **T6** is approximately 21. To explain the lower performance of **T6**, we hypothesize that the sulfur of **T6** reduces the electron deficiency of the carbonyl group *via* the resonance effect. Moreover, the size or polarity of sulfur could also affect substrate binding at the active site of the enzyme. Although **T6** does not perform as well as the native substrate **A6**, this result could be an advantage in HTS because benign variants with small improvements in a library show similar signals to the wild type, which could decrease the numbers of positive hit.

To investigate whether formaldehyde is generated from the reduction of **T6** catalyzed by YahK-WT, the Purpald solution was added after the reaction. After the derivatization, the solution turned purple (Fig. S5b, ESI†), which was further quantified using UV-vis spectroscopy at 550 nm with the calibration curve of a formaldehyde standard solution (Fig. S11, ESI†). Formaldehyde formation was also detected by the Purpald assay in the assays of surrogate reduction catalyzed by DkgA (Fig. S6b, ESI†), YbbO (Fig. S7b and S7d, ESI†), and MAACR (Fig. S8b, ESI†). Furthermore, DTNB was used to quantify the generation of 1-butanethiol after the YahK-WT reaction using the calibration curve of a 1-butanethiol standard solution (Fig. S12, ESI†). From both analyses, the quantities of formaldehyde and 1-butanethiol were nearly stoichiometric with the amount of NADPH consumption (Fig. 1). This suggests that the formyl thioester group of **T6** mimics the aldehyde group to generate formaldehyde after the reductase-catalyzed reaction (Scheme 1). The generated formaldehyde can be derivatized by the Purpald reagent for rapid identification using the naked eye and quantification with UV-vis spectroscopy.

To demonstrate the **T6** feasibility in HTS, we engineered the cofactor specificity of YahK-WT to use NADH because YahK-WT has been reported to have a high preference for NADPH.[16] Therefore, YahK-WT was expressed in *E. coli* MG1655 RARE,[20] where several aldehyde reductase genes including *yahK* were knocked out. The cells were lysed followed by centrifugation to obtain the lysate. As the lysate contains biothiols and different nucleophiles that could probably react with **T6**, the stability of **T6** was also investigated by the incubation of 500 μM of **T6** in the lysate for one hour and then analyzed using DTNB assays. The results showed that **T6** was slightly hydrolyzed to generate about 5% of the hydrolyzed 1-butanethiol in 30 min (Fig. S4, ESI†). Subsequently, further hydrolysis of **T6** was not

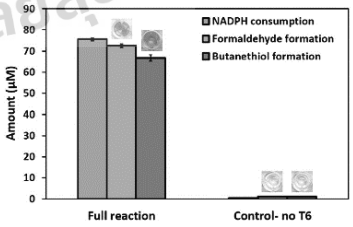

Fig. 1 Reduction of 500 μM **T6** catalyzed by 0.1 μM of purified YahK-WT in the presence of 100 μM NADPH. The results show that NADPH consumption is nearly stoichiometric with the formation of formaldehyde or 1-butanethiol.

Manuscript Chem Comm

(journal impact factor = 6.065)

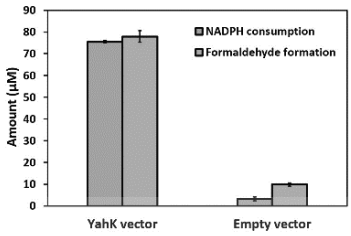

Fig. 2 Reduction of 500 μM of **T6** in the presence of 100 μM of NADPH catalyzed by YahK-WT in lysate. The results show that the NADPH consumption is nearly stoichiometric with formaldehyde formation.

observed, and thus **T6** likely inactivated all the reactive thiols and nucleophiles in the lysate. Furthermore, the **T6** quantity is sufficient for YahK assays. Therefore, 500 μM of **T6** and 100 μM of NADPH were added into the lysate. After 10 min, the Purpald solution was added to derivatize formaldehyde. The solution turned purple as expected. Furthermore, the quantification of NADPH consumption was stoichiometric with the formaldehyde generation (Fig. 2). Therefore, the designed surrogate, **T6**, can be applied in the high throughput screening of FALR engineering.

To decrease the stoichiometric cofactor usage in screening, the cofactor regeneration was incorporated into the assay. Although YahK-WT highly prefers NADPH, it can use NADH with very low activity (Fig. S13, ESI†). To avoid signals from the NADH-dependent reduction, *Pseudomonas* sp. 101 formate dehydrogenase (*Pa*FDH-WT) was chosen as it preferentially reduces NAD^+ to NADH using formate. To test our hypothesis, its variant, *Pa*FDH-V9,[21] which prefers $NADP^+$ was likewise used for comparison. *Pa*FDH-WT or *Pa*FDH-V9 were added into the lysates with the addition of 500 μM of **T6**, 10 mM of formate, and 10 μM of $NADP^+$. After 10 min, the reactions were quenched by the addition of the Purpald solution. The results show that only the assay with *Pa*FDH-V9 turned purple (Fig. S14, ESI†) as YahK-WT prefers NADPH. Hence, *Pa*FDH-WT should be used to regenerate NADH for the cofactor specificity engineering of YahK variants to use NADH (Scheme 2).

To engineer the cofactor specificity of YahK-WT, NADPH was modelled at the active site of YahK-WT using the software AutoDock Vina, which showed that T205 and T206 have a hydrogen bonding interaction with the phosphate group of NADPH (Fig. S15, ESI†). Therefore, the saturation mutagenesis for T205 and T206 was conducted using PCR with the NNK degenerate codon[22] to generate a library of plasmids, which were transformed into *E. coli* MG1655 RARE. Each resulting colony was grown in 96-well plates for YahK variant expression. After cell lysis, the cocktail solution containing 500 μM of **T6**, 10 mM of formate, 500 μM of **T6**, 5 μM of *Pa*FDH-WT, and 10 μM of NAD^+ was added into each well. After 10 min, the Purpald solution was added to quench the reaction and derivatize the generated formaldehyde. Through naked eye observation of a total of 930 variants, numerous positive hits were rapidly identified. The 550 nm absorbance of those hits was further analyzed using the plate reader to identify the two best variants, E3 and C8. According to the sequencing results, the E3 variant contains T206V and the C8 variant contains T205S/T206M. Therefore, their apparent kinetic parameters for NADH and NADPH were determined in the presence of 500 μM of hexanal (**A6**) (Table 1 and Fig. S16, ESI†). The ratio of cofactor specificity ($(k_{cat}/K_m)^{NADH}/(k_{cat}/K_m)^{NADPH}$)[7] is 0.0085 for E3 and 0.0122 for C8 compared with 0.0019 for the wild type. This suggests that E3 and C8 have an improved NADH specificity. The mutations of E3 or C8 disrupt the original hydrogen bonding between the phosphate group of NADPH and T205/T206 due to the hydrophobic residues.

In summary, we designed and successfully synthesized fatty aldehyde surrogates containing the formyl thioester group, which could be reduced by FALRs. The resulting formaldehyde can simply be derivatized by Purpald to form the purple adduct, which is visualized using the naked eye and quantified with UV-vis spectroscopy. Furthermore, the formyl thioester group could be further applied in other surrogate designs for HTS in different reductase engineering purposes.

This work was supported by the Suranaree University of Technology (SUT) and the National Research Council of Thailand (NRCT/PS/132/2563). Suphanida Worakaensai is thankful for the Development and Promotion of Science and Technology Talents Project (DPST) Scholarship. We thank Prof. Kristala Prather for providing the *E. coli* MG1655 RARE, Prof. Brian Pfleger for the MAACR overexpression plasmid, and Prof. Arren Bar-Even for the *Pa*FDH-WT and V9 overexpression plasmids.

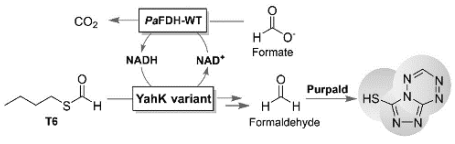

Scheme 2 Assay design with NADH regeneration catalyzed by *Pa*FDH-WT using formate to identify YahK variants utilizing NADH in a library.

Table 1 Apparent kinetic constants[a] of the YahK variants for NADH and NADPH

NADH			
Variant	k_{cat} (s^{-1})	K_m (μM)	k_{cat}/K_m ($\mu M^{-1}/s^{-1}$)
WT	1.63 ± 0.12	245.4 ± 30.9	0.0067 ± 0.0018
E3	3.77 ± 0.20	245.7 ± 22.6	0.0150 ± 0.0028
C8	2.05 ± 0.16	276.4 ± 40.9	0.0074 ± 0.0017
NADPH			
Variant	k_{cat} (s^{-1})	K_m (μM)	k_{cat}/K_m ($\mu M^{-1}/s^{-1}$)
WT	44.50 ± 1.38	12.5 ± 1.8	3.5598 ± 0.6241
E3	116.62 ± 2.34	66.1 ± 4.0	1.7653 ± 0.1410
C8	73.36 ± 3.30	121.0 ± 13.1	0.6061 ± 0.0927

[a] The constants were determined at a fixed concentration of 500 μM of hexanal with varied concentrations of NADH or NADPH catalyzed by the YahK variants.

Manuscript Chem Comm

(journal impact factor = 6.065)

Conflicts of interest

There are no conflicts to declare.

References

1 P. Munkajohnpong, C. Kesornpun, S. Buttranon, J. Jaroensuk, N. Weeranoppanant and P. Chaiyen, *Biofuels, Bioprod. Biorefin.*, 2020, **14**, 986–1009.
2 Q. Yan and B. F. Pfleger, *Metab. Eng.*, 2020, **58**, 35–46.
3 A. Krishnan, B. A. McNeil and D. T. Stuart, *Front. Bioeng. Biotechnol.*, 2020, **8**, 1385.
4 I. J. Cho, K. R. Choi and S. Y. Lee, *Curr. Opin. Biotechnol*, 2020, **65**, 129–141.
5 A. Sharma and S. S. Yazdani, *J. Ind. Microbiol. Biotechnol.*, 2021, **48**, kuab011.
6 P. P. Peralta-Yahya, F. Zhang, S. B. del Cardayre and J. D. Keasling, *Nature*, 2012, **488**, 320–328.
7 A. M. Chánique and L. P. Parra, *Front. Microbiol.*, 2018, **9**, 194.
8 M. J. Vázquez, S. Ashman, F. Ramón, D. Calvo, A. Bardera, J. J. Martín, M. Rüdiger, D. Tew and J. M. Domínguez, *J. Biomol. Screening*, 2005, **11**, 75–81.
9 H. Wu, C. Tian, X. Song, C. Liu, D. Yang and Z. Jiang, *Green Chem.*, 2013, **15**, 1773–1789.
10 S. B. Richard, in *Organic Chemistry of Enzyme-Catalyzed Reactions*, ed. S. B. Richard, Academic Press, San Diego, 2nd edn, 2002, pp. 95–174.
11 M. Mullowney, R. A. McClure, M. T. Robey, N. L. Kelleher and R. J. Thomson, *Nat. Prod. Rep.*, 2018, **35**, 847–878.
12 M. W. Peters, P. Meinhold, A. Anton Glieder and F. H. Arnold, *J. Am. Chem. Soc.*, 2003, **125**, 13442–13450.
13 Y. Yang, Y. T. Chi, H. H. Toh and Z. Li, *Chem. Commun.*, 2014, **51**, 914–917.
14 S. Jonsson, S. Ricagno, Y. Lindqvist and N. G. J. Richards, *J. Biol. Chem.*, 2004, **279**, 36003–36012.
15 Z. P. Gates, J. R. Stephan, D. J. Lee and S. B. H. Kent, *Chem. Commun.*, 2012, **49**, 786–788.
16 G. M. Rodriguez and S. Atsumi, *Metab. Eng.*, 2014, **25** 227–237.
17 R. M. Willis, B. D. Wahlen, L. C. Seefeldt and B. M. Barney, *Biochemistry*, 2011, **50**, 10550–10558.
18 Z. Fatma, K. Jawed, A. J. Mattam and S. S. Yazdani, *Metab. Eng.*, 2016, **37**, 35–45.
19 G. A. Aleku, G. W. Roberts and D. Leys, *Green Chem.*, 2020, **22**, 3927–3939.
20 A. M. Kunjapur, Y. Tarasova and K. L. J. Prather, *J. Am. Chem. Soc.*, 2014, **136**, 11644–11654.
21 L. Calzadiaz-Ramirez, C. Calvó-Tusell, G. M. M. Stoffel, S. N. Lindner, S. Osuna, T. J. Erb, M. Garcia-Borràs, A. Bar-Even and C. G. Acevedo-Rocha, *ACS Catal.*, 2020, **10**, 7512–7525.
22 E. G. Chronopoulou and N. E. Labrou, *Curr. Protoc. Protein Sci.*, 2011, **63**, 26.6.1–26.6.10.

Abstract submitted in The 15th International Symposium of The Protein Society of Thailand

PP055

The surrogate design for high-throughput screening of fatty aldehyde reductases

Suphanida Worakaensai, Surayut Kluaiphanngam, Sirawit Wet-Osot, Utumporn Ngivprom, Anyanee Kamkaew, and Rung Yi Lai*

School of Chemistry, Institute of Science, Suranaree University of Technology, Nakhon Ratchasima 30000, Thailand

***Email:** rylai@sut.ac.th

ABSTRACT

Fatty alcohols are essential industrial raw materials for detergents, plastics, pharmaceuticals, cosmetics, and biofuels. Currently, they are generated from fossil fuels. However, long-term usage of fossil fuels generates lots of concerns, including limited availability and environmental issues associated with global warming, air pollution, etc. In order to mitigate this, researchers conducted synthetic biology to engineer microorganism to produce fatty alcohols. For the synthesis of fatty alcohols, the last step is the reduction of fatty aldehyde to fatty alcohol catalyzed by fatty aldehyde reductase (fatty ALR). To achieve high titer production, the fatty ALR activities require improvement sometimes. The standard approach to characterize their activities is to monitor NADH/NADPH consumption using purified fatty ALR by UV-Vis spectroscopy. However, it takes lots of times for one experiment. Therefore, it is not a suitable method to engineer fatty ALR if the library size is large. In this research, we developed the surrogate of fatty aldehyde containing thioester group. The surrogates could generate formaldehyde, which could be derivatized by purpald to show purple color, after fatty ALR reactions. Therefore, it is promising for whole cell or crude lysate experiments, which are suitable for high throughput screening. We demonstrated few surrogates with different chain lengths on the assays of purified fatty ALR. In the future, we will extend this protocol on high throughput screening of fatty ALR to improve activities for fatty alcohol production.

This research was supported by Thailand Research Fund (MRG6280142).

Abstract submitted in The 34th Annual Meeting of the Thai Society for Biotechnology and International Conference

The 34th Annual Meeting of the Thai Society for Biotechnology and International Conference "Sustainable Bioeconomy : Challenge and Opportunities"

IBP02

High-Throughput Screening using Designed Surrogate for Fatty Aldehyde Reductase Engineering

Suphanida Worakaensai[1], Surayut Kluiphanngam[1], Sirawit Wet-Osot[1], Ratana Charoenwattanasatien[2], Utumporn Ngivprom[1], Chuthamat Duangkamol[1] Anyanee Kamkaew[1], and Rung-Yi Lai[1]*

[1]School of Chemistry, Institute of Science, Suranaree University of Technology, Nakhon Ratchasima 30000, Thailand
[2]Synchrotron Light Research Institute, Nakhon Ratchasima 30000, Thailand
*E-mail: rylai@sut.ac.th

Abstract

Fatty alcohols are essential industrial precursors, such as cosmetics, plastics, and detergents, and are majorly produced from fossil fuels. Long-term usage of fossil fuels generates substantial concerns about fossil fuels depletion and global warming. In order to overcome these, synthetic biology strategies have been used to engineer pathways in microorganisms to produce fatty alcohols. For fatty alcohol biosynthesis, the last step is to reduce a fatty aldehyde to the corresponding fatty alcohol catalyzed by fatty aldehyde reductase (FALR). The activity improvement of FALR is one popular approach to achieving higher yields of fatty alcohol. The standard assay to characterize FALR activities is to monitor NAD(P)H consumption by UV-Vis spectroscopy at 340 nm. This is, however, unsuitable for high-throughput screening (HTS) of FALR engineering because it is labor-intensive and time-consuming. In this work, we developed a novel HTS method using a fatty aldehyde surrogate to test the activity of FALR variants in a library, followed by purpald assay. The hexanal surrogate, T6, containing a formyl thioester group could be reduced by FALR to form formaldehyde as a byproduct. The resulting formaldehyde could be derivatized by purpald to yield a purple adduct, which could be simply visualized by the naked eye or quantified by UV-Vis spectroscopy at 550 nm. To demonstrate the applicability of the screening platform, we successfully applied it to screen *E. coli* YahK library to identify two variants with higher NADH specificity than YahK wild type.

Keywords: Coenzyme engineering; Fatty alcohol; Fatty aldehyde reductase; High-throughput screening

CURRICULUM VITAE

Miss Suphanida Worakaensai was born on April 11th, 1998 in Mukdahan, Thailand. She received her B.Sc. in Biology (first-class honors with a gold medal) in 2019 from the Institute of Science, School of Biology, Suranaree University of Technology, Thailand. She has been granted a scholarship from the Development and Promotion of Science and Technology Talents Project (DPST, THAILAND) since 2016. During her bachelor's degree, she conducted senior research about the effect of nano-hydroxyapatite and calcium on 2-acetyl-1-pyrroline production in rice callus under the supervision of Asst. Prof. Dr. Duangkamol Meansiri. In 2020, she pursued her master's degree program in Biochemistry and Biochemical Technology in the School of Chemistry at the same university with a DPST scholarship. Her master's thesis, which is supervised by Dr. Rung-Yi Lai, focuses on protein engineering by developing high-throughput screening using designed surrogates for fatty aldehyde reductase engineering. She has received a grant from National Research and Innovation Information System (NRIIS, THAILAND) in 2022. Furthermore, she was a research scholar at the Department of Chemical and Molecular Engineering University of California, Irvine, USA under the supervision of Assoc. Prof. Dr. Han Li. She also participated in international conferences (listed in APPENDIX B) during her master's program.